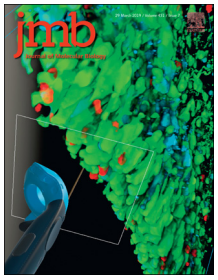

The KN-93 Molecule Inhibits Calcium/Calmodulin-Dependent Protein Kinase II (CaMKII) Activity by Binding to Ca^{2+}/CaM

Melanie H. Wong[1,†], Alexandra B. Samal[2,†], Mike Lee[1], Jiri Vlach[2], Nikolai Novikov[1], Anita Niedziela-Majka[1], Joy Y. Feng[1], Dmitry O. Koltun[1], Katherine M. Brendza[1], Hyock Joo Kwon[1], Brian E. Schultz[1], Roman Sakowicz[1], Jamil S. Saad[2] and Giuseppe A. Papalia[1,]

*1 - **Gilead Sciences Inc,** 333 Lakeside Drive, Foster City, CA 94404, USA*
*2 - **Department of Microbiology,** University of Alabama at Birmingham, Birmingham, AL 35294, USA*

***Correspondence to Jamil S. Saad and Giuseppe A. Papalia:** J.S. Saad is to be contacted at: 845 19th Street South, Birmingham, AL 35294, USA. G.A. Papalia is to be contacted at: Gilead Sciences Inc, 333 Lakeside Drive, Foster City, CA 94404, USA. saad@uab.edu, jpapalia@gilead.com*
https://doi.org/10.1016/j.jmb.2019.02.001
Edited by Patrick Griffin

Abstract

Calcium/calmodulin-dependent protein kinase II (CaMKII) is a multifunctional serine/threonine protein kinase that transmits calcium signals in various cellular processes. CaMKII is activated by calcium-bound calmodulin (Ca^{2+}/CaM) through a direct binding mechanism involving a regulatory C-terminal α-helix in CaMKII. The Ca^{2+}/CaM binding triggers transphosphorylation of critical threonine residues proximal to the CaM-binding site leading to the autoactivated state of CaMKII. The demonstration of its critical roles in pathophysiological processes has elevated CaMKII to a key target in the management of numerous diseases. The molecule KN-93 is the most widely used inhibitor for studying the cellular and *in vivo* functions of CaMKII. It is widely believed that KN-93 binds directly to CaMKII, thus preventing kinase activation by competing with Ca^{2+}/CaM. Herein, we employed surface plasmon resonance, NMR, and isothermal titration calorimetry to characterize this presumed interaction. Our results revealed that KN-93 binds directly to Ca^{2+}/CaM and not to CaMKII. This binding would disrupt the ability of Ca^{2+}/CaM to interact with CaMKII, effectively inhibiting CaMKII activation. Our findings also indicated that KN-93 can specifically compete with a CaMKIIδ-derived peptide for binding to Ca^{2+}/CaM. As indicated by the surface plasmon resonance and isothermal titration calorimetry data, apparently at least two KN-93 molecules can bind to Ca^{2+}/CaM. Our findings provide new insight into how in vitro and *in vivo* data obtained with KN-93 should be interpreted. They further suggest that other Ca^{2+}/CaM-dependent, non-CaMKII activities should be considered in KN-93–based mechanism-of-action studies and drug discovery efforts.

Introduction

Calcium/calmodulin-dependent protein kinase II (CaMKII) is a multifunctional serine/threonine protein kinase that transmits calcium signaling in various cellular processes [1]. Increase in the concentrations of intracellular calcium is sensed by calmodulin (CaM), which in turn promotes activation of CaMKII [2]. There are four known isozymes of CaMKII (α, β, γ, and δ) [3]. In the brain, CaMKIIα is intimately related to memory and learning [4]. A role for CaMKII has also been implicated in epilepsy [5] and depression [6]. In myocardial tissue, CaMKIIδ has been linked to arrhythmia [7,8] as well as remodeling due to atrial fibrillation and myocardial infarction [8–10]. A protective role for CaMKIIδ has been implicated in ischemia/reperfusion [11,12]. Given these latter associations, CaMKIIδ remains a target of high interest in cardiovascular disease [13].

CaMKIIα and δ holoenzymes have been shown to exist in a dodecameric state [14–17]. X-ray crystallography studies have shown that in the inactive inhibited state, a regulatory α-helix binds to the substrate binding pocket of CaMKII [14,17]. Electron

paramagnetic resonance data suggest that the CaM-binding region of this α-helix is in equilibrium between a docked and undocked state, primed for Ca^{2+}/CaM to bind [18]. When the concentration of intracellular calcium increases, Ca^{2+}/CaM binds to this regulatory α-helix, releasing it from the substrate binding pocket [17]. Upon binding of Ca^{2+}/CaM, the α-helix adopts an extended conformation that interacts with an adjacent catalytic domain within the dodecamer, leading to the trans-phosphorylation of critical threonine residues proximal to the site of CaM binding which contributes to the auto-activated state of CaMKII [17]. This autophosporylation event leads to the high-affinity binding of Ca^{2+}/CaM, also called "CaM trapping" [19]. In the absence of phosphorylation and nucleotide, binding of Ca^{2+}/CaM is expected to be relatively weak [17,20].

Various small-molecule inhibitors of CaM/CaMKII activation have been characterized, among them, KN-93 (*N*-[2-[*N*-(4-chlorocinnamyl)-*N*-methylaminomethyl]phenyl]-*N*-(2-hydroxyethyl)-4-methoxybenzenesulfonamide) (Fig. 1) [21]. Interestingly, discovery of KN-93 arose from studies of W7 (*N*-(6-aminohexyl)-5-chloronaphthalene-1-sulfonamide, Fig. 1), characterized as a CaM antagonist [22–24]. Subsequent to the generation of W7, further synthetic efforts led to the replacement of the naphthalene group with isoquinoline to generate a class of isoquinilonesulfonamides [25]. KN-62 (1-[*N*,*O*-bis(5-isoquinolinesulfonyl)-*N*-methyl-L-tyrosyl]-4-phenylpiperazine), a later generation and more chemically elaborate isoquinilonesulfonamide (Fig. 1), also marked the discovery of an inhibitor of CaMKII activation [26]. In searching for a more soluble version of KN-62, Hidaka and co-workers [21] synthesized KN-93 (Fig. 1). Like KN-62, KN-93 was able to inhibit Ca^{2+}/CaM-dependent activation of CaMKII and to be competitive with Ca^{2+}/CaM [21]. The authors were unable to show a direct interaction between Ca^{2+}/CaM and KN-93 in affinity chromatography experiments and concluded that the binding site on KN-93 resided on CaMKII. Interestingly, HMN-709 (2-[*N*-(2-aminoethyl)-*N*-(4-chlorobenzenesulfonyl)]amino-*N*-(4-fluorocinnamyl)-*N*-methylbenzylamine), a molecule that is structurally very similar to KN-93 (Fig. 1), has been shown to bind Ca^{2+}/CaM [27]. Broadly speaking, KN-62, KN-93, HMN-709, and the known CaM antagonists W7

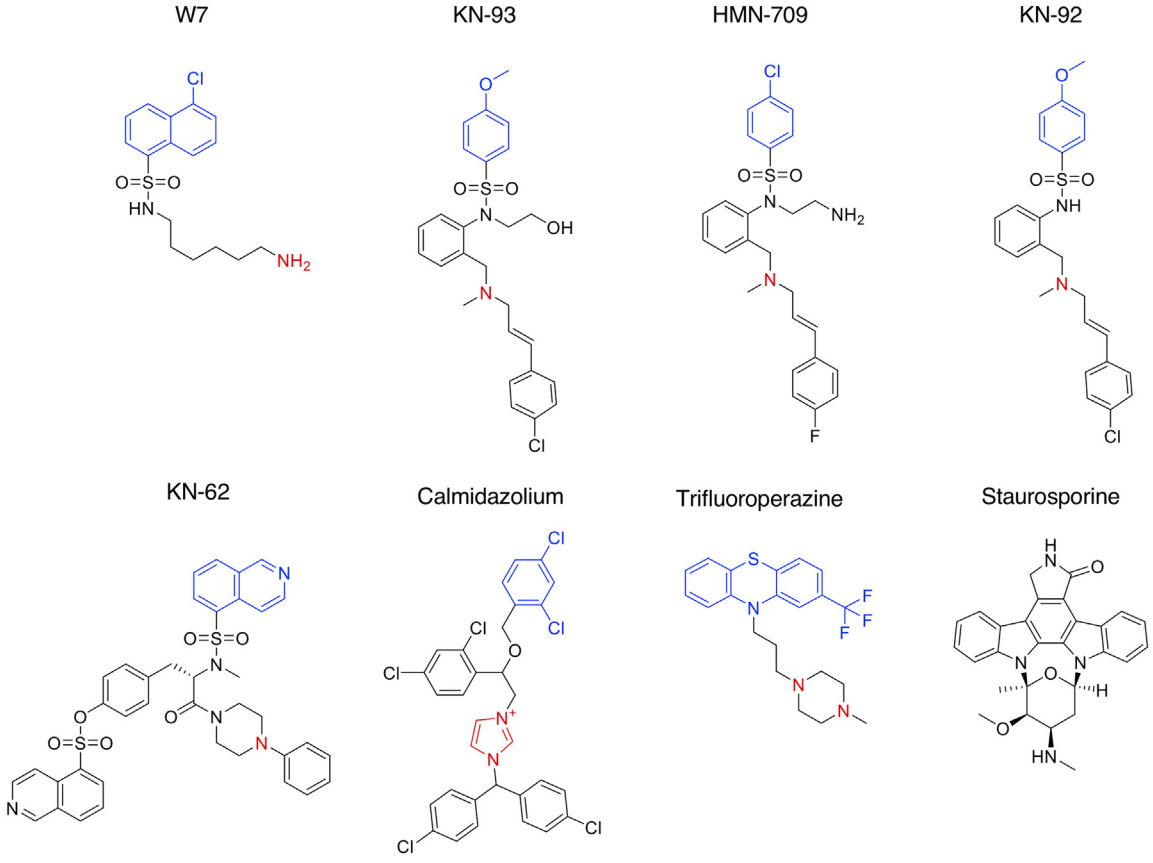

Fig. 1. Chemical structures of known small-molecule inhibitors of Ca^{2+}/CaM or CaMKII FL. The common aryl sulfonamide moieties in W7, KN-93, HMN-709, KN-92, and KN-62, or general aryl moieties in TFP and calmidalzolium are shown in blue. The moiety responsible for the positive charge at physiological pH is shown in red; either a basic nitrogen or the imidazolium group as in calmidazolium. Staurosporine is a well-established kinase inhibitor that was used in this study.

[22–24], calmidazolium [28–30], and trifluorperazine [31–33] all have certain pharmacophoric features in common (Fig. 1); they all contain an aryl moiety and a positive charge resulting from the protonation of a basic nitrogen at physiological pH, or in the case of calmidazolium, a permanent positive charge. KN-92, closely related in its features to KN-93 (Fig. 1), is considered an inactive analog [8,13,34].

A major unresolved question is how KN-93 acts to inhibit CaM-dependent activation of CaMKII. It is widely accepted that KN-93 is a CaMKII inhibitor implicating this enzyme in many cellular processes, with some researchers even suggesting that KN-93 may be effective therapeutically in humans [35]. Herein, we employed surface plasmon resonance (SPR), NMR, isothermal titration calorimetry (ITC), and enzymatic assays to elucidate the molecular basis of CaMKII inhibition by KN-93. We have chosen to study the δ isoform of CaMKII since many of the uses of KN-93 come from studies of the heart or myocytes [8,10,12,36–38] where this isoform predominates. We demonstrate that KN-93 binds directly to Ca^{2+}/CaM and not to monomeric or dodecameric constructs of CaMKIIδ, a finding with significant implications for the interpretation of data from both *in vitro* and *in vivo* use of KN-93.

Results

KN-93 binds directly to Ca^{2+}/CaM

Enzymatic studies were performed to reproduce the expected inhibitory behavior of KN-93 [21] and also to compare IC_{50} values with direct binding data from SPR studies (see below). These enzymatic studies used a TR-FRET assay that monitored the phosphorylation of a substrate peptide (Materials and Methods). Proteins were prepared as described in Materials and Methods. The dodecameric status of CaMKIIδ was confirmed by analytical ultracentrifugation (Fig. S1). Calmidazolium, a known Ca^{2+}/CaM antagonist [28–30], and staurosporine, a widely used protein kinase inhibitor [39] were used as controls. Inhibition curves for calmidazolium, staurosporine, and KN-93 using monomeric CaMKIIδ (referred to as $CaMKII\delta_{Monomer}$ hereafter) and dodecameric CaMKIIδ (hereafter referred to as $CaMKII\delta_{Dodecamer}$) are shown in Fig. 2. $CaMKII\delta_{Monomer}$ is based on the sequence of a human CaMKIIδ construct lacking the oligomerization domain and has been previously characterized by x-ray crystallography [17]. This construct is monomeric in the crystal structure and shows only a weak dimer association in solution [17]. For each compound, fitted values of IC_{50} using both $CaMKII\delta_{Monomer}$ and $CaMKII\delta_{Dodecamer}$ are within 3-fold of each other (Fig. 3 and Table 1). This result confirms that KN-93 is able to inhibit CaMKIIδ enzymatic activity, and that it does so for both $CaMKII\delta_{Monomer}$ and $CaMKII\delta_{Dodecamer}$. We were unable to determine whether KN-93 binds to Ca^{2+}/CaM or to CaMKIIδ using an enzymatic approach (Fig. S2). However, the IC_{50} values obtained from enzymatic experiments (Table 1) allowed for a direct comparison with K_d values obtained from direct binding studies (see below) ensuring that surface- and solution-based studies yielded values that were in agreement.

Next, we used the ProteOn XPR36 SPR protein interaction array system to assess the direct binding of KN-93, calmidazolium, and staurosporine to CaM, $CaMKII\delta_{Monomer}$, and $CaMKII\delta_{Dodecamer}$. The small-molecule binding activity of the Ca^{2+}/CaM surface was validated by the finding that this surface was competent to bind calmidazolium in a calcium-dependent manner (Fig. 4A). The observed K_d of 100 nM (Table 2) was similar to IC_{50} values obtained from the enzymatic studies using either $CaMKII\delta_{Monomer}$ or $CaMKII\delta_{Dodecamer}$ (110 and 70 nM, respectively; Table 1). These IC_{50} values agree with the range of previously published values obtained for the inhibition by calmidazolium of several Ca^{2+}/CaM–dependent enzymes (between 10 nM and 5 μM [30]). The ability of $CaMKII\delta_{Monomer}$ and $CaMKII\delta_{Dodecamer}$ surfaces, as well as small molecules to interact as expected was validated using staurosporine (Fig. 4B). The high-affinity interaction observed (K_d = 0.39 nM for $CaMKII\delta_{Monomer}$ and K_d = 0.28 nM for $CaMKII\delta_{Dodecamer}$; Table S1) is consistent with previously published data (K_d = 0.32 nM) for staurosporine and CaMKIIδ [39], and also with the high potency of this molecule observed in the enzymatic studies using either $CaMKII\delta_{Monomer}$ or $CaMKII\delta_{Dodecamer}$ (IC_{50} = 0.11 and 0.06 nM, respectively; Table 1). When KN-93 was injected at concentrations as high as 100 μM, little or no response was observed on the $CaMKII\delta_{Monomer}$ or $CaMKII\delta_{Dodecamer}$ surfaces (Fig. 4C). Since staurosporine and KN-93 have comparable molecular masses (466 and 501 Da, respectively), binding of KN-93 to either $CaMKII\delta_{Monomer}$ or $CaMKII\delta_{Dodecamer}$ should have led to a response comparable to that observed for staurosporine binding to these surfaces. However, binding of KN-93 was clearly observed on the Ca^{2+}/CaM surface and only in the presence of calcium (Fig. 4C). As expected [8,13,34], KN-92 did not show evidence of specific binding even when using concentrations of KN-92 as high as 100 μM (data not shown). As with K_d values obtained for calmidazolium and staurosporine, the K_d observed for KN-93 binding directly to Ca^{2+}/CaM (6 μM) agreed with the IC_{50} values obtained from enzymatic data (9 and 3 μM using $CaMKII\delta_{Monomer}$ and $CaMKII\delta_{Dodecamer}$, respectively; Tables 1 and 2). While the close agreement between IC_{50} and K_d values obtained from enzymatic and SPR studies

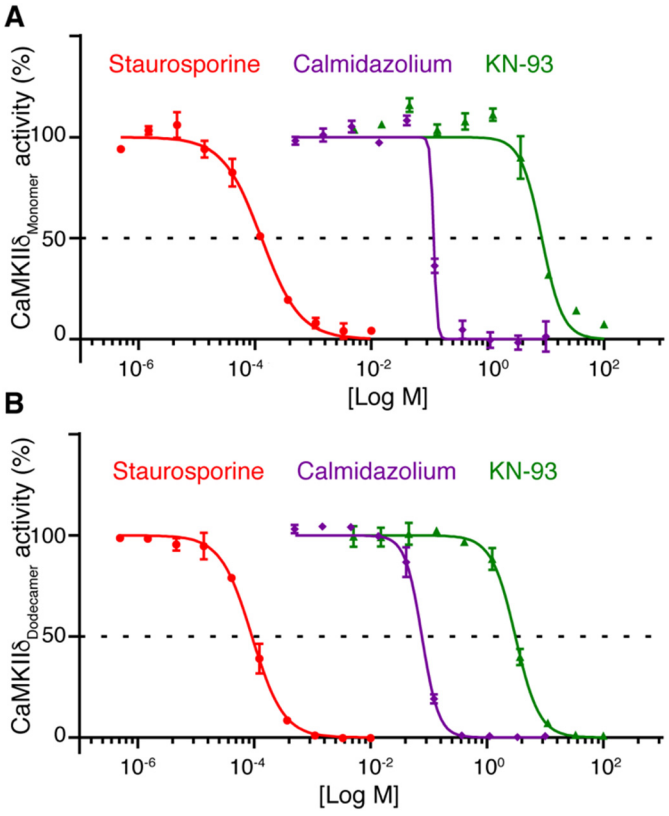

Fig. 2. Representative inhibition curves of $CaMKII\delta_{Monomer}$ and $CaMKII\delta_{Dodecamer}$ activity by various small molecules. Inhibition of $CaMKII\delta_{Monomer}$ (A) and $CaMKII\delta_{Dodecamer}$ (B) activities by staurosporine, the CaM antagonist calmidazolium, and KN-93. Error bars in the figure represent standard deviations calculated from duplicate measurements in a single experiment using Prism. Averaged parameters from these fits were obtained from three independent experiments as shown in Table 1.

indicates that these two methods are reporting on the same interaction phenomena, the SPR data indicate that KN-93 inhibition observed enzymatically is due to the direct binding of KN-93 to Ca^{2+}/CaM, and not to $CaMKII\delta_{Monomer}$ or $CaMKII\delta_{Dodecamer}$.

Attempts to further validate the Ca^{2+}/CaM surface by showing $CaMKII\delta_{Monomer}$ binding to Ca^{2+}/CaM were complicated by a binding profile that indicated complex kinetics, that is, a profile having more than one phase in the association and/or dissociation phase (Materials and Methods and Figs. S3 and S4). Instead, we utilized three CaMKIIδ-derived peptides of various lengths: a 13-, 17-, and 22-mer (and hereafter referred to as short, intermediate, and long) to validate the Ca^{2+}/CaM surface. The sequences of these peptides are derived from the Ca^{2+}/CaM-binding region of CaMKIIδ and correspond to residues 301–313 (KGAILTTMLATRN), 297–313 (RRKLKGAILTTMLATRN), and 292–313 (KKFNARRKLKGAILTTMLATRN) of the human CaMKIIδ sequence. Interactions of these peptides with Ca^{2+}/CaM have been previously characterized by ITC methods [40]. Unlike the interaction profile with $CaMKII\delta_{Monomer}$, binding of the three peptides with Ca^{2+}/CaM could be modeled using a simple kinetic model with a term added to account for mass transport when necessary (Materials and Methods). The Ca^{2+}/CaM–peptide interactions are all calcium-dependent, and the peptides displayed a range of affinities for Ca^{2+}/CaM (Fig. 5A–C, Tables 2 and S1) consistent with previously published data [40,41]. Together with the observed response to calmidazolium, these observations demonstrate the binding competency of the Ca^{2+}/CaM surfaces used and, by extension, further validate the binding of KN-93 to Ca^{2+}/CaM.

KN-93 competes with a Ca^{2+}/CaM-binding peptide

Next, we performed competition experiments to determine whether the inhibitor molecules could compete with the CaMKIIδ intermediate peptide for binding to Ca^{2+}/CaM. In these experiments, peptide at a single concentration (1 nM) was mixed with various defined concentrations of KN-93 or calmidazolium and then injected over the Ca^{2+}/CaM surface. Data for all injections were globally fit to a simple competition model in which both peptide and inhibitor compete for the same binding site on Ca^{2+}/CaM (see Materials and Methods). For ease of visualization, competition data and fits from a single surface are shown for selected concentrations only of KN-93 and calmidazolium (Fig. 6). SPR data show that KN-93 (Fig. 6A) and calmidazolium (Fig. 6B) compete with 1 nM intermediate peptide for binding to Ca^{2+}/CaM. At low concentrations of KN-93 or calmidazolium where little competition is expected (Fig. 6A and B, respectively), the sensorgrams show a nearly monophasic slow dissociation, consistent with surface Ca^{2+}/CaM being bound predominantly

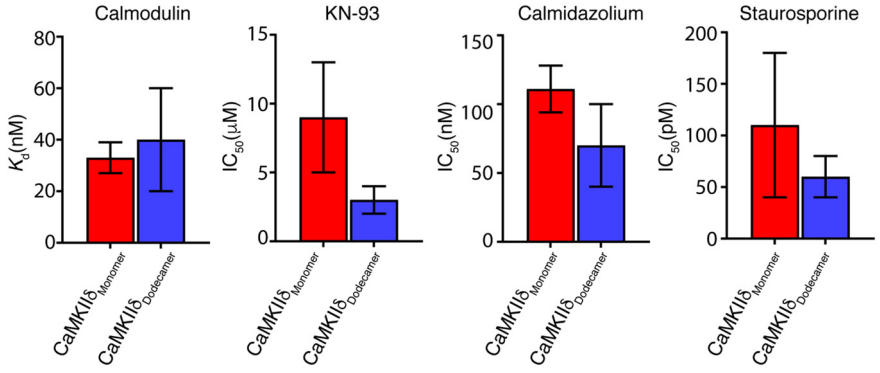

Fig. 3. Bar graph representation of K_d and IC_{50} values from Table 1 for molecules inhibiting CaMKIIδ$_{Monomer}$ and CaMKIIδ$_{Dodecamer}$ activity. Data show that both protein forms behave similarly in enzymatic experiments. Error bars represent 95% confidence intervals.

by the peptide. In contrast, at higher concentrations of KN-93 or calmidazolium, two dissociation phases were observed; fast and slow, suggesting two populations of dissociating species from surface Ca^{2+}/CaM. Initially, a fast dissociation phase is observed, attributable to the faster dissociations observed for KN-93 and calmidazolium. This is followed by a slow phase, attributable to the dissociation of intermediate peptide. Fitting of these competition data sets as described above converged to solutions yielding parameters (denoted as $K_{d\text{-Competition}}$, $k_{on\text{-Competition}}$ and $k_{off\text{-Competition}}$; Table 2) within experimental error of those obtained from direct binding experiments ($K_{d\text{-Direct}}$, $k_{on\text{-Direct}}$ and $k_{off\text{-Direct}}$; Table 2), with the minor exception of $K_{d\text{-Direct}}$ and $K_{d\text{-Competition}}$ for calmidazolium whose lower and upper bounds for K_d differ modestly ($K_{d\text{-Direct}}$ = 80 nM, $K_{d\text{-Competition}}$ = 52 nM). We also note that the ratio of response factors (cited as the ratio of peptide to small-molecule *R*-factor in Table 2) obtained for intermediate peptide to small molecule is 1.0 ± 0.1 and 0.7 ± 0.2 for KN-93 and calmidazolium, respectively (Table 2). For 1:1 stoichiometry, this ratio is expected to be ~4 since the mass of the intermediate peptide is ~4 times that of KN-93 and calmidazolium; thus, the lower obtained values suggest the binding of approximately four molecules of KN-93 or calmidazolium to one molecule of Ca^{2+}/CaM (see Materials and Methods for more details). Interestingly, a stoichiometry of 4–6 molecules of calmidazolium binding to a synthetic construct of Ca^{2+}/CaM has been noted previously [42]. The possibility of KN-93 binding to Ca^{2+}/CaM with a stoichiometry greater than 1:1 was examined further by ITC methods (see below). Overall, the demonstrated ability of KN-93 to compete with a CaMKIIδ-derived peptide ties the direct binding of KN-93 to Ca^{2+}/CaM with the original observation that this molecule can inhibit CaMKII activation [21].

Binding properties of KN-93 to Ca^{2+}/CaM as detected by NMR

NMR chemical shifts are very sensitive to variations in the local molecular environment. Small changes in the ^{1}H and ^{15}N resonances obtained by collecting two-dimensional (2D) ^{1}H–^{15}N heteronuclear single quantum coherence (HSQC) spectra on protein–ligand complexes can be used to map the binding interface. These experiments allow for identification of not only residues involved in the interaction but also those involved in accompanying conformational changes. To examine how KN-93 binds to Ca^{2+}/CaM and to identify the interaction interface, we obtained 2D ^{1}H–^{15}N HSQC data on a uniformly ^{15}N-labeled Ca^{2+}/CaM upon titration with KN-93. As observed in Fig. 7A,

Table 1. Enzyme kinetic parameters and inhibition constants for selected inhibitors against CaMKIIδ$_{Monomer}$ and CaMKIIδ$_{Dodecamer}$

	CaMKIIδ$_{Monomer}$	CaMKIIδ$_{Dodecamer}$
Specific activity (nmol phosphopeptide/min/mg protein)[a]	150 ± 20	310 ± 40
CaM Apparent K_d (M)	$3.3 \pm 0.6 \times 10^{-8}$	$4 \pm 2 \times 10^{-8}$
ATP K_m (M)	$2.2 \pm 0.5 \times 10^{-4}$	$6 \pm 2 \times 10^{-5}$
KN-93 IC_{50} (M)	$9 \pm 4 \times 10^{-6}$	$3 \pm 1 \times 10^{-6}$
Calmidazolium IC_{50} (M)	$1.1 \pm 0.2 \times 10^{-7}$	$7 \pm 3 \times 10^{-8}$
Staurosporine IC_{50} (M)	$1.1 \pm 0.7 \times 10^{-10}$	$6 \pm 2 \times 10^{-11}$

Errors denote 95% confidence intervals as calculated from a minimum of three experiments, with the exception of ATP K_m values where errors denote standard deviations calculated from two experiments; values from these two experiments differed less than 2-fold.

[a] Measured at saturating CaM, 140 μM ATP, and 1 μM peptide substrate.

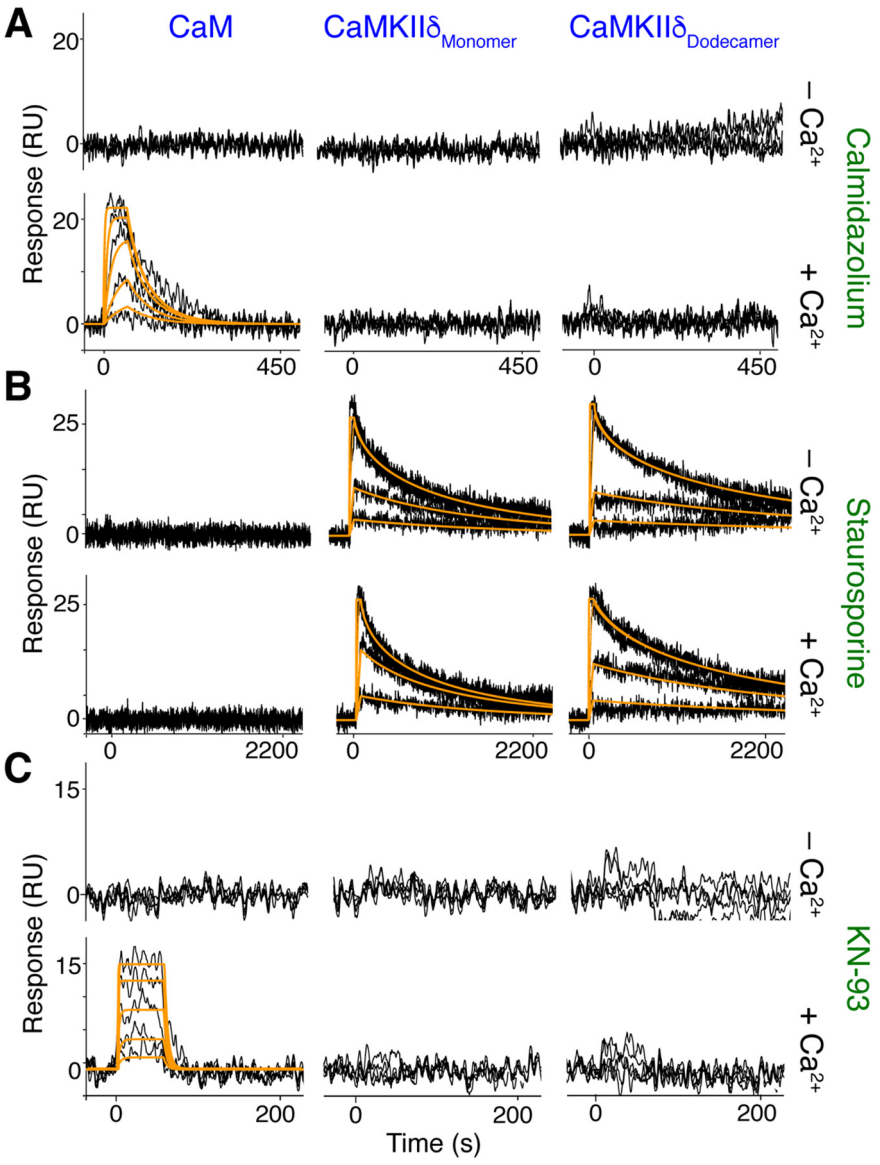

Fig. 4. Calcium dependence and small-molecule binding to CaM, $CaMKII\delta_{Monomer}$ and $CaMKII\delta_{Dodecamer}$. Injections of the analytes (A) calmidazolium, (B) staurosporine, and (C) KN-93 over surfaces of CaM, $CaMKII\delta_{Monomer}$, or $CaMKII\delta_{Dodecamer}$ in the absence and presence of 2 mM calcium (top and bottom panels, respectively, for each analyte). Data (black lines) were fit with a simple kinetic model (orange line). Parameters obtained from these are shown in Table 2 and Table S1.

numerous signals exhibited significant CSPs upon the addition of KN-93. Chemical shift changes ceased at 3:1 KN-93:Ca^{2+}/CaM consistent with a saturable binding event. Interestingly, the affected residues are spread throughout the N- and C-terminal lobes of Ca^{2+}/CaM (Fig. 7B). As indicated by the CSPs, a subset of signals are in fast exchange on the NMR time scale between the free and bound forms of Ca^{2+}/CaM. Other $^{1}H–^{15}N$ signals exhibited a decrease in intensity accompanied by appearance of several new signals, consistent with intermediate-to-slow exchange on the NMR time scale between the free and bound forms of Ca^{2+}/CaM. The presence of two exchange regimes in the NMR spectra may indicate binding of more than one KN-93 molecule and/or induction of an allosteric conformational change. It is noteworthy that slow and fast exchange regimes have also been observed upon binding of trifluoperazine (TFP) to CaM and indicated binding of up to four TFP molecules [43]. Consistent with the SPR data, NMR titrations of Ca^{2+}/CaM with the inactive KN-92 analog indicated very weak binding (data not shown).

Next, we conducted similar NMR experiments on the ^{15}N-labeled $CaMKII\delta_{Monomer}$ sample as titrated with KN-93. The number of $^{1}H–^{15}N$ resonances in the HSQC spectrum of CaMKII matches the number of residues. As shown in Fig. S5, no detectable changes have been observed upon the addition of excess

Table 2. Interaction parameters derived from direct binding and competition SPR experiments with Ca^{2+}/CaM

	Direct binding[a]			Peptide competition data[a]			
	$k_{on\text{-}Direct}$ (M^{-1} s^{-1})	$k_{off\text{-}Direct}$ (s^{-1})	$K_{d\text{-}Direct}$ (M)	$k_{on\text{-}Competition}$ (M^{-1} s^{-1})	$k_{off\text{-}Competition}$ (s^{-1})	$K_{d\text{-}Competition}$ (M)	Peptide/small-molecule *R*-factor
KN-93	$2 \pm 2 \times 10^{4}$[b]	$1.3 \pm 0.3 \times 10^{-1}$	$6 \pm 3 \times 10^{-6}$	$3 \pm 1 \times 10^{4}$	$1.0 \pm 0.1 \times 10^{-1}$	$4 \pm 2 \times 10^{-6}$	1.0 ± 0.1
Calmidazolium	$3 \pm 2 \times 10^{5}$	$3 \pm 2 \times 10^{-2}$	$1.0 \pm 0.2 \times 10^{-7}$	$2.8 \pm 0.1 \times 10^{5}$	$1.39 \pm 0.07 \times 10^{-2}$	$5.0 \pm 0.2 \times 10^{-8}$	0.7 ± 0.2
Intermediate peptide (direct)	[c]	[c]	$4 \pm 3 \times 10^{-11}$				
Intermediate peptide (from competition with KN-93)[d]				$7 \pm 10 \times 10^{7}$[b]	$3 \pm 4 \times 10^{-3}$[b]	$4 \pm 2 \times 10^{-11}$	1.0 ± 0.1
Intermediate peptide (from competition with Cz)[d]				$1.6 \pm 0.8 \times 10^{7}$	$4 \pm 2 \times 10^{-4}$	$2.2 \pm 0.5 \times 10^{-11}$	0.7 ± 0.2

[a] Numbers with errors denote average values obtained from three independent experiments. Fitting from each independent experiment involved the global fitting of 2–3 surface densities. Errors denote the 95% confidence interval of the average. All other values in the table have been cited to two significant digits. Fitting of the competition data of intermediate peptide by KN-93 and calmidazolium also included simultaneously fitting of the respective direct binding data for KN-93 or calmidazolium performed in the same experiment (see Materials and Methods).

[b] Lower bound of confidence interval could not be determined with sufficient precision.

[c] Kinetics could not be reliably determined due to mass transport; K_d value obtained from Scrubber 2.0 software.

[d] Kinetics derived from competition of intermediate peptide with KN-93 or calmidazolium (Cz).

amounts of KN-93, indicating no direct binding. In comparison, addition of the kinase inhibitor staurosporine into a ^{15}N-labeled CaMKII$\delta_{Monomer}$ sample led to dramatic chemical shift changes in the HSQC spectrum, demonstrating direct staurosporine binding to CaMKII$\delta_{Monomer}$ (Fig. S6). Altogether, our NMR data show that KN-93 binds directly to Ca^{2+}/CaM and not to CaMKIIδ.

Mode of KN-93 binding to Ca^{2+}/CaM. Role of the N- and C-terminal hydrophobic lobes

To gain more insights into the mode of KN-93 binding to Ca^{2+}/CaM, we devised two approaches. First, we titrated KN-93 into ^{15}N-labled samples of Ca^{2+}/CaM-N (residues 1–80) and Ca^{2+}/CaM-C (residues 76–148) followed by acquisition of 2D ^{1}H–^{15}N HSQC NMR data. A subset of ^{1}H–^{15}N signals exhibited significant CSPs upon titration of KN-93 into Ca^{2+}/CaM-N (Fig. 8A and B). The CSPs in the HSQC spectra indicate fast exchange, on the NMR time scale, between the free and bound forms. Mapping of the KN-93 binding site on the Ca^{2+}/CaM-N structure show that KN-93 binds to a well-defined pocket formed by hydrophobic residues, including methionines (Met) (Fig. 8C). On the other hand, addition of substoichiometric amounts of KN-93 to ^{15}N-labeled Ca^{2+}/CaM-C (0.5:1 KN-93:Ca^{2+}/CaM-C) led to a decrease in intensity for a significant number of ^{1}H–^{15}N resonances accompanied by appearance of several new signals, consistent with a slow exchange on the NMR time scale between the free and bound forms. A steady decrease in intensity for the original ^{1}H–^{15}N signals and increase in intensity of the new signals was observed with further addition of KN-93. Spectral changes ceased at 1:1 KN-93:Ca^{2+}/CaM-C (Fig. 8A). As shown in Fig. 8A and B, CSPs are pronounced throughout the NMR spectrum. Mapping of the KN-93 binding site on the Ca^{2+}/CaM-C structure also revealed a pocket formed by several hydrophobic residues including Met residues (Fig. 8C). However, compared to Ca^{2+}/CaM-N, CSPs appear to be more substantial and are mapped to a larger surface of Ca^{2+}/CaM-C, suggesting that KN-93 may have induced a conformational change. Of note, the observation of two exchange regimes in the HSQC spectra upon titration of KN-93 to full-length Ca^{2+}/CaM is consistent with binding of two KN-93 molecules to the two hydrophobic lobes. These results indicate that KN-93 binds with a higher affinity to the C-domain of CaM than it does to the N-domain, which is consistent with other CaM antagonists such as TFP [43,44].

In the second approach, we assessed the role of hydrophobic surfaces located on the N- and C-terminal lobes of Ca^{2+}/CaM. These hydrophobic surfaces contribute to the flexibility and function of Ca^{2+}/CaM [45]. Structural studies have established that calcium binding induces a helical rearrangement, leading to exposure of eight Met residues [46,47]. It has been shown that Met residues are

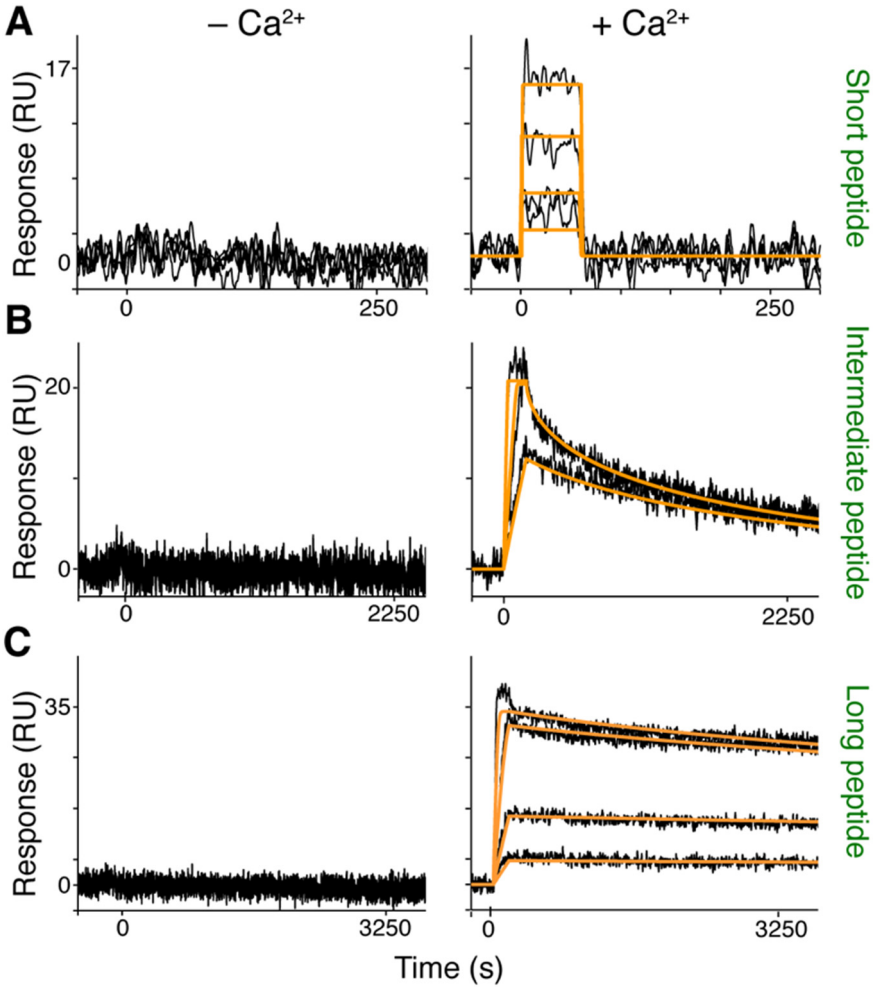

Fig. 5. Calcium dependence and binding of CaMKIIδ-derived peptides to CaM. Injection of (A) short, (B) intermediate, and (C) long CaMKIIδ-derived peptides over CaM surfaces in the absence (left panels) and presence (right panels) of 2 mM calcium. Data (black lines) for the short peptide were fit with a simple kinetic model (orange lines); a mass transport term was added for the fitting of the intermediate and long peptides. Parameters obtained from these fits are shown in Table 2 and Table S1.

essential for the unique promiscuous binding behavior of Ca^{2+}/CaM to target proteins and ligands [47]. The methyl groups of Met residues (Cε) are useful "NMR reporters" and have been used to probe for binding of target proteins/peptides and inhibitors [47–54]. To further assess whether the N- and C-terminal hydrophobic surfaces contribute to binding, we collected 2D $^{1}H–^{13}C$ HMQC data on a uniformly ^{13}C-labeled Ca^{2+}/CaM sample as titrated with KN-93 (Fig. S7). Addition of a substoichiometric amount of KN-93 (0.5:1 KN-93:Ca^{2+}/CaM) led to the disappearance of $^{1}H–^{13}C$ signals of Met^{51}, Met^{71}, Met^{72}, Met^{109}, Met^{124}, and Met^{145} (Fig. S7). At saturation (3:1 KN-93:Ca^{2+}/CaM), only five $^{1}H–^{13}C$ signals were detectable. Severe broadening and/or loss of Met Cε NMR signals is possibly caused by an intermediate chemical exchange process involving the two ligands. Taken together, our NMR data indicate that both the N- and C-terminal lobes of Ca^{2+}/CaM are involved in KN-93 binding and that the hydrophobic surfaces formed by Met residues contribute to binding.

Thermodynamics of KN-93 binding to Ca^{2+}/CaM

The NMR data above suggest that KN-93 binds to both of the N-terminal and C-terminal lobes of Ca^{2+}/CaM. However, it was difficult to assess the stoichiometry of the interaction between KN-93 and Ca^{2+}/CaM from the NMR data because of the two different exchange regimes on the NMR time scale. To determine the stoichiometry and other thermodynamic parameters, we obtained ITC data upon titration of KN-93 into Ca^{2+}/CaM. ITC provides values for K_d, stoichiometry of binding (n), enthalpy change (ΔH°) and the entropic term ($T\Delta S^\circ$). As shown in Fig. 9A, binding of KN-93 to Ca^{2+}/CaM is exothermic as indicated by the sign of the enthalpy.

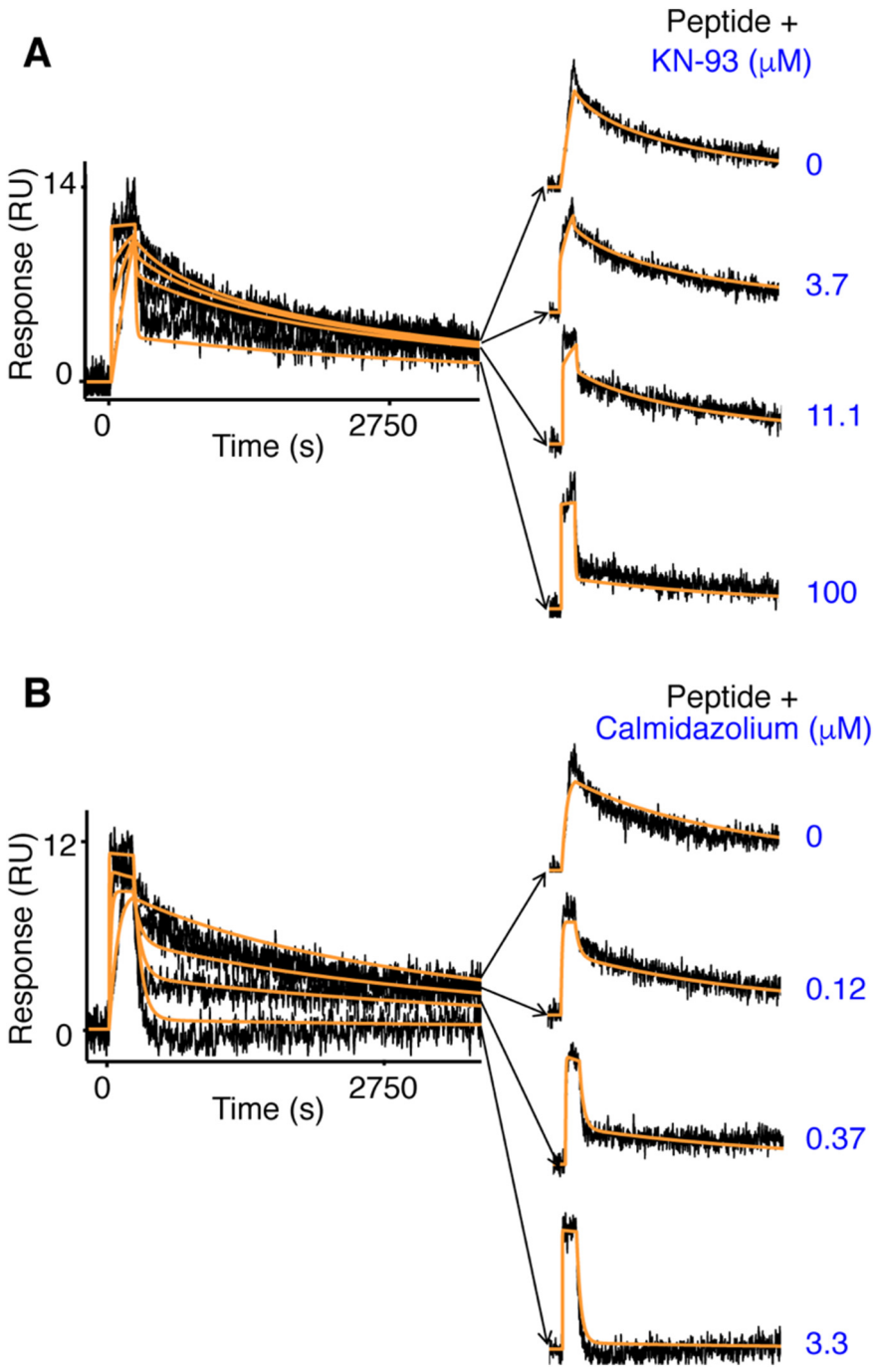

Fig. 6. Competition studies with KN-93 or calmidazolium and intermediate peptide for binding to Ca^{2+}/CaM surfaces. Intermediate peptide at a concentration of 1 nM alone or in the presence of (A) various concentrations of KN-93 or (B) calmidazolium over a Ca^{2+}/CaM surface. Data (black lines) for all injections are globally fit with a simple competition model (orange lines) where both peptide and KN-93 (or calmidazolium) compete for the same binding site on Ca^{2+}/CaM. Parameters derived from these fits from three independent experiments are shown in Table 2.

By fitting the binding data to a single set of identical sites, the following parameters were obtained: K_d = 380 ± 71 nM, n = 2.1 ± 0.02, ΔH° = −7.7 ± 0.18 kcal/mol, and $-T\Delta S^\circ$ = −0.8 ± 0.2 kcal/mol. Our ITC data show that two KN-93 molecules bind to Ca^{2+}/CaM. As indicated by the enthalpy and entropy values, both ionic and slightly favorable hydrophobic interactions may contribute to the formation of the Ca^{2+}/CaM–KN-93 complex. On the other hand, ITC experiments conducted upon

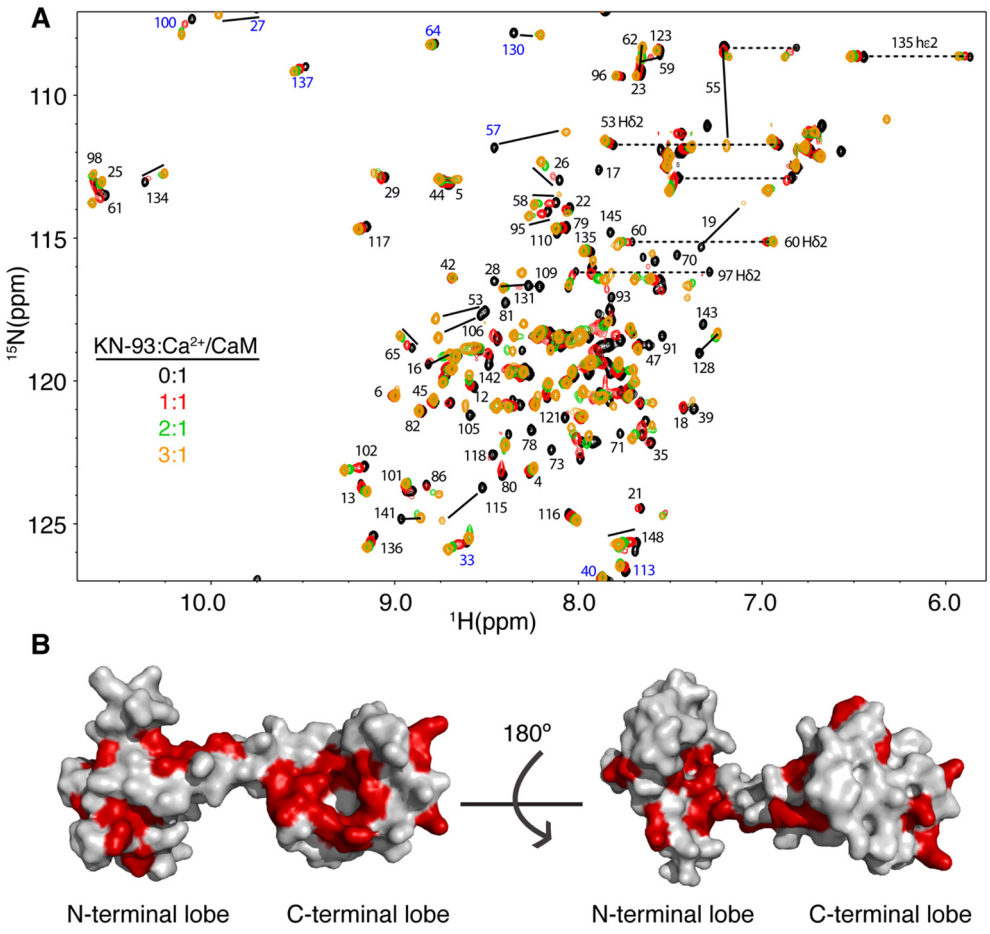

Fig. 7. NMR data and chemical shift mapping of KN-93 binding to Ca^{2+}/CaM. (A) Overlay of 2D ^{1}H–^{15}N HSQC spectra upon titration of a 100 μM sample of Ca^{2+}/CaM with KN-93. Signal labels correspond to residues of CaM in the bound form. Signals labeled in blue are shifted by 20 ppm due to aliasing. Dashed lines denote side-chain amide signals. (B) Surface representation of the CaM structure (PDB ID: 3CLN) highlighting residues (red) that exhibited significant chemical shift changes upon binding of KN-93. Figures were generated by Pymol (The PyMOL Molecular Graphics System, Schrödinger, LLC).

titration of KN-93 into $CaMKII\delta_{Monomer}$ protein yielded no detectable binding (Fig. 9B). Consistent with the SPR and NMR data, ITC results indicate that KN-93 does not bind to $CaMKII\delta_{Monomer}$. Altogether, our SPR, NMR, and ITC data provide definitive evidence for a direct interaction between KN-93 and Ca^{2+}/CaM, a result that has significant consequences for studies using KN-93.

Methionine to glutamine substitutions in CaM abolish KN-93 binding

To further elucidate the mode of KN-93 binding to Ca^{2+}/CaM and to assess the role of Met residues in binding, we used site-directed mutagenesis to change key methionine residues to glutamines. This substitution introduced a polar amide group at the same position in the side chain as the original sulfide. It is expected that the greater polarity of the Gln side chain relative to Met will decrease the hydrophobic interactions of Ca^{2+}/CaM with KN-93. Furthermore, Met-to-Gln substitution does not significantly disturb the structure of Ca^{2+}/CaM because both amino acids are structurally similar and possess similar propensity to form α-helices. Met-to-Gln substitutions have been previously utilized to study Ca^{2+}/CaM interactions with target proteins [55,56]. Herein, we generated two full-length CaM mutant constructs in which Met residues in the N-terminal lobe (M71/M72/M76) and in the C-terminal lobe (M109/M124/M144/M145) were substituted with Gln. Proteins were expressed and purified as described for the wild-type CaM protein. Next, we obtained ITC data upon titration of KN-93 into both mutant Ca^{2+}/CaM proteins. As shown in Fig. S8, titration of KN-93 yielded thermograms that are significantly different from that obtained for the wild-type Ca^{2+}/CaM protein (Fig. 9A). For the Ca^{2+}/CaM (M71Q/M72Q/M76Q) mutant, the titration data were fit with a model having a single set of identical sites and yielded the following parameters: K_d = 2.9 ± 0.8 μM, n = 0.93 ± 0.04, ΔH° = −5.1 ±

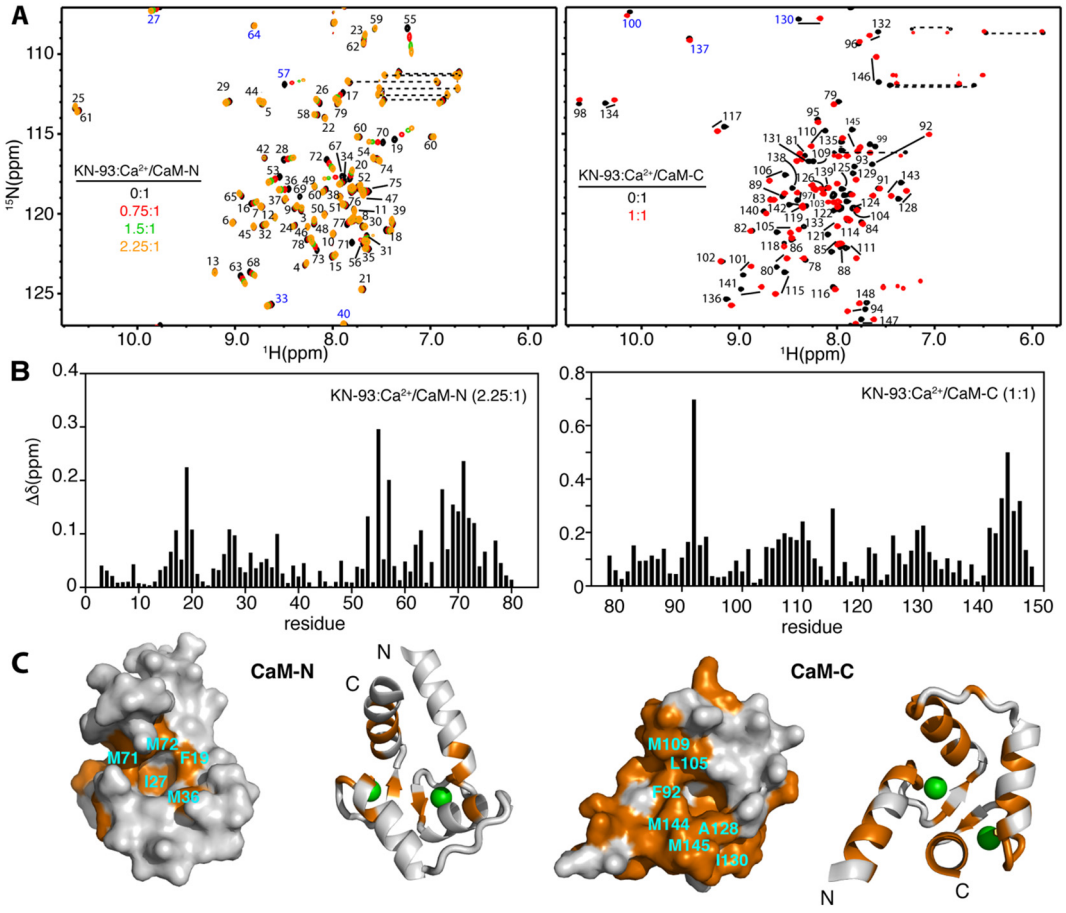

Fig. 8. NMR data and chemical shift mapping of KN-93 binding to Ca^{2+}/CaM-N and Ca^{2+}/CaM-C. (A) Overlay of 2D $^{1}H–^{15}N$ HSQC spectra upon titration of KN-93 into Ca^{2+}/CaM-N and Ca^{2+}/CaM-C. Signals labeled in blue are shifted by 20 ppm due to aliasing. Dashed lines denote side-chain amide signals. (B) Histograms of normalized $^{1}H–^{15}N$ chemical shift changes *versus* residue number calculated from the HSQC spectra for Ca^{2+}/CaM-N and Ca^{2+}/CaM-C upon titration with KN-93. (C) Cartoon and surface representations of Ca^{2+}/CaM-N and Ca^{2+}/CaM-C lobes (PDB ID: 3CLN) highlighting residues (orange, with cyan labels) that exhibited significant chemical shift changes upon KN-93 binding. Green spheres represent calcium ions. Figures were generated by Pymol.

0.4 kcal/mol, and $-T\Delta S^{\circ} = -2.4 \pm 0.2$ kcal/mol. For the Ca^{2+}/CaM (M109Q/M124Q/M144Q/M145Q) mutant, the following parameters were obtained: $K_d = 4.8 \pm 1.6$ μM, $n = 1.1 \pm 0.1$, $\Delta H^{\circ} = -6.7 \pm 0.8$ kcal/mol, and $-T\Delta S^{\circ} = -0.6 \pm 0.5$ kcal/mol. Importantly, in both cases, the stoichiometry of binding is ~1:1, indicating that Met-to-Gln substitutions in either of the N- or C-terminal lobes abrogated binding of KN-93 to that domain. Consistent with the NMR observations, these results indicate that KN-93 binds to both lobes of Ca^{2+}/CaM. In addition, as indicated by the K_d values, the affinity of KN-93 to either of the mutants decreased by ~10-fold. This result is interesting as it suggests that Met-to-Gln substitution in one lobe affects the binding affinity of KN-93 to the other. A possible explanation for this finding is the presence of some cross-talk between the two lobes when KN-93 binds, a possibility not captured in fits of KN-93 titrations with wild-type Ca^{2+}/CaM.

Discussion

KN-93 has been described as an allosteric inhibitor of CaM/CaMKII activity [13]. The first characterization of KN-93 concluded that this molecule was competitive for Ca^{2+}/CaM binding to CaMKII, but via its direct binding to CaMKII, not Ca^{2+}/CaM [21]. Herein, we critically assessed the binding mode of KN-93 to CaMKIIδ and Ca^{2+}/CaM using various techniques. We provided definitive evidence of direct binding of KN-93 (and also calmidazolium) to Ca^{2+}/CaM but were unable to detect binding of KN-93 to $CaMKII\delta_{Monomer}$ or $CaMKII\delta_{Dodecamer}$ constructs. There is consistency in these results since KN-93 and calmidazolium, like other small molecules known to bind Ca^{2+}/CaM such as HMN-709 [27], W7 [49], and TFP [43], all contain an aryl moiety and a positive charge resulting from the protonation of a basic nitrogen at physiological

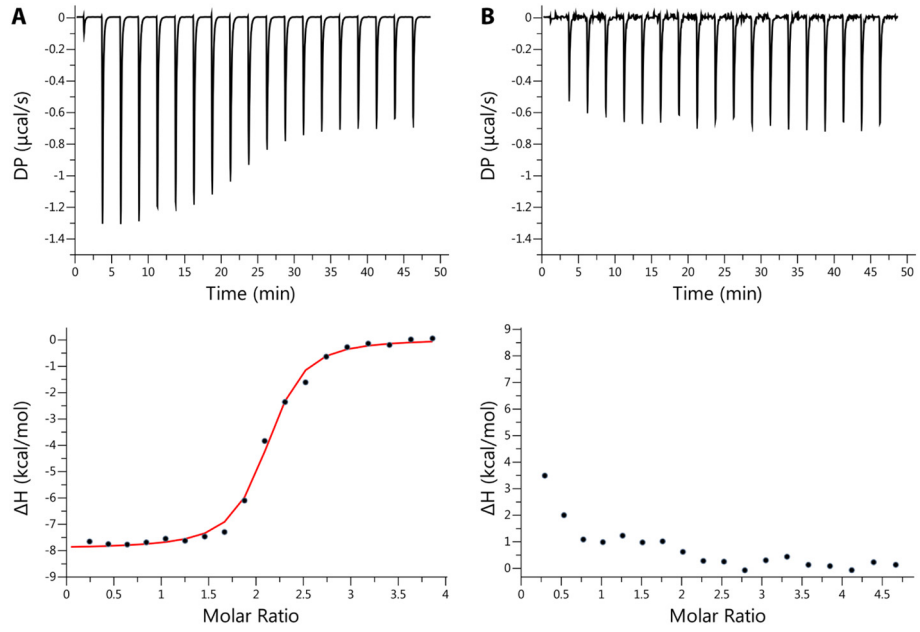

Fig. 9. ITC data of KN-93 binding to Ca^{2+}/CaM or $CaMKII\delta_{Monomer}$. (A) ITC thermogram recorded upon injections of KN-93 (400 µM) into Ca^{2+}/CaM (20 µM). Fits of the data yielded a stoichiometry of two KN-93 molecules bound to Ca^{2+}/CaM (n = 2.1 ± 0.02). (B) ITC thermograms recorded upon injections of KN-93 (411 µM) to $CaMKII\delta_{Monomer}$ (17 µM). Binding to $CaMKII\delta_{Monomer}$ was not detected.

pH, or in the case of calmidazolium, a permanent positive charge. This pharmacophoric feature for molecules known to bind Ca^{2+}/CaM has been noted previously and even predates the synthesis of KN-93 [57].

The inhibition experiments presented here were effectively modeled by invoking a simple competitive model whereby KN-93 or calmidazolium competes with peptide for the same binding site on Ca^{2+}/CaM. Despite this, predicting the actual site for KN-93 binding to CaM is not straightforward. Existing data of Ca^{2+}/CaM binding to $CaMKII\delta_{Monomer}$ [17], W7 [31], and TFP [31–33] show that numerous residues located in the N- and C-terminal domains of Ca^{2+}/CaM can be involved. We have shown that one KN-93 molecule binds to the N- and C-terminal lobe each of Ca^{2+}/CaM. In particular, the hydrophobic surfaces formed by the Met residues on both lobes are critical for KN-93 binding. We have shown that substitution of Met residues in the N- or C-terminal lobes abolishes binding of KN-93 to that lobe. Previous structural studies revealed that W7 and TFP bind to Ca^{2+}/CaM with different modes. Whereas one W7 molecule binds to each hydrophobic pocket on the N- and C-terminal lobes of CaM [49], controversy still surrounds the mode of TFP binding to Ca^{2+}/CaM. Three x-ray structures revealed that one, two, or four TFP molecules are capable of binding to Ca^{2+}/CaM [31–33]. NMR studies have also suggested that four TFP molecules can bind to Ca^{2+}/CaM [43]. The binding affinity of the first TFP molecule is, however, suggested to be significantly higher than the additional molecules [31]. This precedence for super-stoichiometric binding of small molecules to Ca^{2+}/CaM is certainly in line with our own stoichiometric data for KN-93 and also calmidazolium.

ITC and SPR studies suggested stoichiometries of 2:1 and ~ 4:1, respectively, for KN-93 binding to Ca^{2+}/CaM. Since SPR is sensitive to the refractive index increment of molecules [58], and since small molecules can show significant differences in their refractive index increment (dn/dc) [59] compared to proteins, one possible source for this discrepancy would be if the dn/dc value for KN-93 was twice that for the intermediate peptide. This would result in twice the expected response for small molecule than for intermediate peptide. However, there was no difference observed in dn/dc values for KN-93 and intermediate peptide (see Materials and Methods). It is possible that the conformation of immobilized Ca^{2+}/CaM lends itself to the capture of more KN-93 molecules. Of course, there may be unknown variables between these two experimental platforms that remain unappreciated. Further investigation of the binding mode of KN-93 to Ca^{2+}/CaM is warranted. We also note that the affinity of KN-93 to Ca^{2+}/CaM obtained from ITC studies (K_d ~370 nM) is ~14-fold tighter than that obtained from SPR studies (K_d ~5 µM). Discrepancies in Ca^{2+}/CaM K_d's for both the intermediate and long peptide between platforms (e.g., ITC and fluorescence) has been observed previously [40]. Discrepancies in those studies were ascribed to using

different versions of CaM and the different platforms used. It is possible that the need to biotin-label Ca^{2+}/CaM in our own SPR studies may be a contributing factor to the differences in affinity observed in ITC and SPR. Matrix effects have also been shown to be a source of discrepancies in solution- and surface-based platforms [60].

Although the mode of action we present remains consistent with KN-93 being regarded as a functional inhibitor of CaMKII, the ubiquity of Ca^{2+}/CaM naturally leads to questions of whether some KN-93-based observations are explained as well, if not better by a mode of inhibition that is Ca^{2+}/CaM-dependent but CaMKII-independent. For instance, previous reports relying on effects observed with KN-93 have linked CaMKII activity to both L-type calcium channels and potassium channel activity responsible for the outward potassium current in myocytes [36–38]. In some of these studies [36,37], KN-93 was able to mediate effects on potassium current even while CaMKII activity was inhibited by CaMKII-inhibitory peptides. These results led investigators to propose the possibility of CaMKII-independent mechanism for KN-93 [36,37]. A CaMKII-independent mechanism is in fact plausible since there is now broad and compelling evidence that Ca^{2+}/CaM can interact directly with various ion channels [61]. Together with the findings in this work, this suggests that in addition to regulation of channel activity by CaMKII phosphorylation, the direct inhibition by KN-93 of Ca^{2+}/CaM binding to these channels should also be considered in explaining these observations.

The consideration of CaMKII-independent pathways may also help to harmonize observations between various mouse studies. Previous work using KN-93 implicated a protective activity for CaMKII in myocardial infarction induced by ischemic reperfusion [12]. However, work with a genetic CaMKIIδ knockout mouse has called these conclusions into question [62]. The possibility that KN-93 may inhibit other kinases such as protein kinase D, a kinase implicated in pathological cardiac remodeling [63], has been cited as a possible reason for this discrepancy. Given our findings, the possible inhibition of a kinase such as protein kinase D is entirely plausible since this kinase is also a member of the Ca^{2+}/CaM-dependent group of serine/threonine protein kinases [64] and therefore also subject to inhibition via an interaction with KN-93 and Ca^{2+}/CaM.

We have shown that KN-93 binding to CaM is calcium-dependent. The degree to which initial KN-93 binding is linked to conformational changes in CaM will therefore be tied to the degree of bound calcium. Of course, further conformational changes upon binding of KN-93 are possible. The clearest picture of conformational changes will have to await elucidation of KN-93–Ca^{2+}/CaM complex structure.

Finally, it is possible that KN-93 may bind other targets. The caution required in interpreting data using KN-93 has been noted previously [8,65]. Interestingly, studies on the effect of KN-92 and KN-93 on ion channel activity [66,67] show that KN-92 is also able to inhibit activity. This KN-93/KN-92 activity profile is different than that observed with Ca^{2+}/CaM and suggests a target for KN-93 and KN-92 other than Ca^{2+}/CaM in some settings. Our own analysis has provided an understanding of KN-93 activity in a specific molecular context, that of its binding to Ca^{2+}/CaM and lack thereof toward the δ-isoform of CaMKII. Continued investigation using the biophysical approaches outlined herein should help elucidate other outstanding questions regarding this molecule.

Materials and Methods

Reagents and proteins

Staurosporine, calmidazolium, KN-92, water-soluble KN-93, and EZ-Link-NHS-LCLC biotin were purchased from LC Laboratories, EMD Millipore, Cayman Chemical, Abcam Biochemicals, and ThermoFisher Scientific, respectively. Short (Ac-KGAILTTMLATRN-NH_2), intermediate (Ac-RRKLKGAILTTMLATRN-NH_2), and long peptides (Ac-KKFNARRKLKGAILTTMLATRN-NH_2) were custom synthesized by GenScript. BSA was obtained from Cell Signaling Technology (Danvers, MA). For dn/dc measurements, KN-93 and the intermediate CaMKIIδ peptide were reconstituted in water at concentrations of 2.0 and 9.15 mg/mL. dn/dc values for KN-93 and intermediate CaMKIIδ peptide were assessed on an Agilent 1260 HPLC system (Agilent Technologies, Santa Clara, CA) with the RI detector of an OMNISEC REVEAL multi-detector system. The HPLC column used was a Zenix SEC-100, 4.6 × 300 mm, 3 μm (Sepax Technologies, Newark, DE) with water as mobile-phase and sample solvent (Milli-Q A10; Millipore Sigma, Burlington, MA), with flow at 0.2 mL/min and injection volumes ranging from 3 to 50 μL. Calibration was performed with the dextran 73 K standard, (dn/dc = 0.147) at 2.433 mg/mL (Malvern Panalytical, Malvern, UK). OMNISEC v10 software was used to obtain dn/dc values for both KN-93. dn/dc values for KN-93 and intermediate CaMKIIδ peptide obtained were 0.03 ± 0.01 (n = 2) and 0.033 ± 0.007 (n = 3).

Human CaM (residues 2–149) for enzymatic and SPR experiments was generated by PCR from a plasmid containing a cDNA for CaM (Origine). The PCR product was ligated into petDuet. Full-length human CaM used in enzymatic and SPR experiments was overexpressed in *Escherichia coli* without any affinity tag. Cells were lysed in Buffer A

[50 mM Hepes (pH 7.5), 40 mM NaCl, and 10% glycerol] and centrifuged at 40,000*g*. The supernatant was passed through an anion exchange column pre-equilibrated with Buffer A. CaM was eluted using a linear gradient [50 mM Hepes (pH 7.5), 1 M NaCl, and 10% glycerol]. The fractions containing CaM were pooled, ammonium sulfate was added to 1.5 M, and the mixture was loaded on a hydrophobic interaction chromatography (HIC) Phenyl HP column. CaM weakly bound to the HIC column was obtained during the wash step [50 mM Hepes (pH 7.5), 1.5 M $(NH_4)_2SO_4$, and 10% glycerol]. This relatively pure protein was further purified using size exclusion chromatography in 50 mM Hepes (pH 7.5), 300 mM NaCl, 10% glycerol, and 1 mM $CaCl_2$. Purity of the CaM sample was confirmed by SDS-PAGE, and the identity of the protein was confirmed by mass spectrometry (see below, for more information on mass spectrometry methods).

The $CaMKII\delta_{Monomer}$ gene (human CaMKIIδ residues 11–335) used in SPR experiments was generated by PCR from a plasmid containing a cDNA for CaMKIIδ (ATCC). The PCR product was ligated into pET28a containing an N-terminal His-tag cleavable with TEV protease. CaMKIIδ protein co-expressed with lambda phosphatase in BL21 codon plus RIPL cells. Cells were lysed in 50 mM Hepes (pH 7.5), 150 mM NaCl, and 10 mM DTT. The $CaMKII\delta_{Monomer}$ protein was purified using Ni-NTA affinity chromatography with a linear imidazole gradient. The His-tag was removed with TEV protease and uncleaved protein was separated by Ni-NTA affinity chromatography. Fractions containing $CaMKII\delta_{Monomer}$ were pooled, concentrated, and further purified by size exclusion chromatography in a buffer containing 50 mM Hepes (pH 7.5), 150 mM NaCl, and 10 mM DTT. The $CaMKII\delta_{Monomer}$ construct used in enzymatic experiments was generated in a similar manner. The PCR product was ligated into pET30a containing a C-terminal His-tag cleavable with TEV protease. The protein was purified as described above. The identity of the proteins was confirmed by mass spectrometry (see below, for more information on mass spectrometry methods).

Human CaMKIIδ (residues 2–478), corresponding to the full-length sequence of the dodecamer, used in enzymatic and SPR experiments was generated by PCR from a plasmid containing a cDNA for CaMKIIδ (NCBI accession number NP_742113.1; ATCC). The PCR product was ligated into pFASTBac containing an N-terminal His-tag. Full-length human CAMKIIδ was expressed in Sf21 insect cells. The cell pellet was resuspended in buffer B [25 mM Tris–HCl (pH 8.5), 300 mM NaCl, and 2 mM tris(2-carboxyethyl)phosphine (TCEP)] supplemented with 1× Complete EDTA free protease inhibitor cocktail (Roche Applied Science) and 1% (w/v) *n*-tetradecylphosphocholine (FC14). FC14 was found to improve yield and solubility of full-length CAMKIIδ and was maintained throughout purification. Cells were lysed using a dounce homogenizer, and the lysate was clarified by centrifugation at 40,000*g* for 1 h. The protein-containing supernatant was loaded onto a Ni-NTA HP column, which was washed first with buffer C [buffer B supplemented with 0.01% (w/v) FC14], then washed with buffer C supplemented with 75 mM imidazole (pH 8.5). The protein was then eluted with buffer C supplemented with 250 mM imidazole (pH 8.5). The fractions containing full-length CAMKIIδ were pooled, diluted, and then loaded onto an anion exchange column, which was then washed with buffer D [25 mM Tris–HCl (pH 8.5), 100 mM NaCl, 2 mM TCEP, and 0.01% (w/v) FC14]. Protein was eluted using a linear gradient to 0.5 M NaCl. The fractions containing CAMKIIδ were pooled and further purified by size exclusion chromatography in a buffer containing 25 mM Tris–HCl (pH 8.5), 300 mM NaCl, 5 mM TCEP, and 0.01% (w/v) FC14. The oligomeric state (dodecamer) was confirmed by analytical ultracentrifugation (Fig. S1).

Identity of the CaM, $CaMKII\delta_{Monomer}$, and $CaMKII\delta_{Dodecamer}$ constructs was confirmed by intact mass spectrometry using an Agilent 6210 Time of Flight Mass Spectrometer and an Agilent 1200 Rapid Resolution HPLC. The samples were analyzed on an Agilent Zorbax 300 Extend C18 Rapid Resolution column at 70 °C, using reverse phase chromatography with a gradient from 20 to 90% acetonitrile containing 0.1% formic acid. Data were analyzed using Agilent Masshunter B.06 Qualitative Analysis with the Bioconfirm upgrade.

Enzymatic assay

The enzymatic integrity of expressed Ca^{2+}/CaM as well as $CaMKII\delta_{Monomer}$ and $CaMKII\delta_{Dodecamer}$ CaMKIIδ was assessed by reproducing the expected inhibition profiles of KN-93, calmidazolium, and staurosporine. Solutions of CAMKIIδ (final concentration for $CaMKII\delta_{Dodecamer}$ and $CaMKII\delta_{Monomer}$ enzymes were at 40 and 80 pM, respectively), the proprietary biotinylated peptide substrate STK1 (final concentration of 1 μM; CisBio, MA), CaM (present at a concentration 2× apparent K_d for IC_{50} determinations), and inhibitor were prepared in an assay buffer containing 20 mM Hepes (pH 7.2), 10 mM $MgCl_2$, 1 mM $CaCl_2$, 1 mM DTT, 0.1% Tween20, and 1% dimethyl sulfoxide (DMSO). After a 30-min preincubation to allow for equilibration of inhibitor binding, ATP was added to a final concentration of 140 μM to start the reaction. The reaction volume was 100 μL. After a 12-min reaction to measure initial rates, the reaction was quenched with 50 μL of 3× quench/detection solution (CisBio) containing a Eu-labeled anti-phosphopeptide antibody and a TR-FRET acceptor molecule XL-665 conjugated with

streptavidin. After mixing overnight at room temperature, the plate was read using a Tecan Infinite M1000 plate reader in a time-resolved fluorescence resonance energy transfer mode, with an excitation wavelength of 317 nm and detection wavelengths of 620 and 665 nm. The ratio of emission at 665 nm/620 nm was used as the measure of product formation. In all enzymatic experiments, less than 5% of the substrate was consumed over the time course of the reaction. There was no loss of enzyme activity observed over the time course of the enzymatic experiments. This assay has been previously used to identify potent inhibitors of CaMKII that are highly potent in rat ventricular myocytes, selective against hERG, and other off-target kinases and that also display good CaMKII tissue selectivity (cardiac δ/γ *versus* neuronal α/β) [68]. All enzymatic parameters obtained are listed in Table 1. $CaMKII\delta_{Monomer}$ and $CaMKII\delta_{Dodecamer}$ constructs showed very similar apparent K_d values for Ca^{2+}/CaM (33 ± 6 and 40 ± 20 nM, respectively), and K_m values for ATP were within four-fold of each other (220 and 60 μM, respectively). IC_{50} values obtained using $CaMKII\delta_{Monomer}$ and $CaMKII\delta_{Dodecamer}$ for binding of calmidazolium (110 ± 20 and 70 ± 30 nM, respectively), staurosporine (110 ± 70 and 60 ± 20 pM, respectively), and KN-93 (9 ± 4 and 3 ± 1 μM, respectively) were also similar. Based on standard enzymatic competition studies performed with both $CaMKII\delta_{Dodecamer}$ and $CaMKII\delta_{Monomer}$ proteins, KN-93 was characterized as competitive with Ca^{2+}/CaM binding. However, this behavior could arise from KN-93 binding to the CaMKII enzyme, or KN-93 binding directly to Ca^{2+}/CaM. Our experiments were not able to differentiate between the two possibilities (Fig. S2).

SPR studies

Label-free binding studies were performed on a ProteOn XPR36 using GLM chips. Immobilizations were performed according to standard protocol from the ProteOn amine coupling kit (Bio-Rad, Hercules, CA) to obtain approximately 12, 500 RU of neutravidin. Captured proteins were minimally biotinylated [69] in running buffer containing 50 mM Hepes (pH 7.4), 150 mM NaCl, 2 mM $CaCl_2$, 10 mM $MgCl_2$, 1 mM TCEP, 0.001% Brij-35, and 1% DMSO. Biotinylation proceeded using a 1:1 stoichiometric ratio of EZ-Link-NHS-LCLC biotin to protein at 4 °C for 1 h and in the presence of 100 μM of KN-93 to protect any putative KN-93 binding sites in the constructs. KN-93 and excess biotin were removed using 0.5-mL Zeba desalting columns with a 7-kDa molecular weight cutoff (ThermoFisher Scientific). The presence of only one major biotin peak in these constructs was confirmed via mass spectrometry. CaMKIIδ constructs and CaM were captured in the vertical direction and at densities allowing for a maximum binding response (R_{max}) of ~15–50 RU. Surfaces were blocked with two pulses of 50 μM amine PEG biotin. Concentration series of small molecules or peptides were injected in the horizontal direction for a specified contact time. Dissociation times were optimized to collect sufficient dissociation profiles. All compounds were injected at a flow rate of 100 μL/min. Calcium dependence was assessed by capturing proteins and injecting analytes prepared with running buffer containing 2 mM ethylene glycol-bis(β-aminoethyl ether)-*N*,*N*,*N*′,*N*′-tetraacetic acid (EGTA). We noted possible differences in the magnitude of analyte response when surfaces had been exposed to running buffer containing EGTA first and then supplemented with calcium, compared to responses on surfaces that had been exposed only to buffers containing calcium. To allow for direct comparison, all parameters cited in Table 2 are derived from surfaces of CaM not previously treated with EGTA. Data were referenced and corrected for DMSO solvent effects and drift using the ProteOn Manager software (version 3.1.0.6; Bio-Rad). Since some data sets required modeling using CLAMP XP2 software (competition fits, see below), all data collected from the ProteOn XPR36 were exported and fit using CLAMP XP2 software (Biologic Software Pty Ltd) [70]. Direct binding data were fit using a simple kinetic model and included a mass transport term [71–73] when necessary. For all figures, data were first smoothed using a smoothing function in CLAMP and then exported to Excel.

Preliminary binding experiments injecting $CaMKII\delta_{Monomer}$ over immobilized Ca^{2+}/CaM to help validate the Ca^{2+}/CaM surface were difficult to analyze due to a complex kinetic profile (Fig.S3A–C). The profiles could be ameliorated by addition of BSA to the buffers (Fig. S4A). Although the fits to these sensorgrams are not fully optimal (see below for a possible contributing factor), the sensorgrams are consistent with affinities in the 1-μM range and in agreement with other affinities reported for Ca^{2+}/CaM binding to autoinhibited isolated kinase domains [17], and unphosphorylated CaMKII in the absence of nucleotide [20]. However, competition experiments led to negative sensorgram responses; this is especially visible with calmidazolium (Fig. S4C). Dose-dependent negative sensorgrams that can be fit and that are consistent with saturable responses have been noted previously [74,75]; however, their origin remains obscure. Given the mechanistic intent of this work and absence of a complete understanding of the interactions leading to this observation, we used peptides (described above) to validate the Ca^{2+}/CaM surface and also to perform competition experiments (see below). The biophysical binding properties of these peptides to Ca^{2+}/CaM have been previously characterized [40], and we have found these peptides to not require use of BSA in the running buffer.

To assess the ability of KN-93 or calmidazolium to compete with intermediate peptide binding to Ca^{2+}/CaM, mixtures of 1 nM intermediate peptide containing either 0, 1.2, 3.7, 11, 33, or 100 μM of water-soluble KN-93 were injected over Ca^{2+}/CaM surfaces. The intermediate peptide was chosen because its affinity was compatible with the concentrations of KN-93 and calmidazolium required to observe competition, and because its kinetic profile was distinct from that of KN-93 and calmidazolium. KN-92 was also tested using the same concentration range. A 10-fold lower concentration series (0, 0.12, 0.37, 1.1, 3.3, and 10 μM) was used for calmidazolium. Mixtures were injected for 240 s using flow rates of 100 μL/min and monitored for a dissociation time of 3600 s. Data for all injections were globally fit to a simple competition model where both peptide (A) and KN-93 or calmidazolium (A′) compete for the same binding site on Ca^{2+}/CaM (B). Data were fit to the following equations:

1. $A0 \rightleftarrows A$
2. $A + B \rightleftarrows AB$
3. $A' + B \rightleftarrows A'B$

where A0 is the concentration of intermediate peptide in the bulk and A is the concentration of intermediate peptide on the surface. The first equation was included since intermediate peptide binding to Ca^{2+}/CaM is mass-transport limited in its kinetics. Since 2–3 densities from each experiment were fit, values of R_{max} for KN-93 or calmidazolium binding to Ca^{2+}/CaM were fit locally. Global parameters fitted include k_{on} and k_{off} for A and A′, and the *R*-factors, also known as response factors for AB and A′B. *R*-factors relate the magnitude of response expected for different analytes due primarily to their mass; their ratio can be thought of as the ratio of R_{max}'s expected between AB and A′B. R_{max} information for the intermediate peptide species is limited in these experiments because it is injected at only one concentration and also because its kinetics are affected by mass transport. In order to provide the competition fitting with as much R_{max} information as possible for at least one of the analytes, fitting of the competition data of intermediate peptide by KN-93 and calmidazolium also included simultaneously fitting of the respective direct binding data for KN-93 or calmidazolium performed in the same experiment; the solution was further constrained by fixing the *R*-factor for A′B (i.e., the small molecule) to 1.

Ratios of the peptide to small-molecule *R*-factors obtained are provided in Table 2. Since the mass of intermediate peptide is 1984 Da and that of calmidazolium and KN-93, 652 and 501 Da, respectively, the ratio of theses *R*-factors is expected to be ~3–4 for stoichiometries of 1:1. In fact, the ratios obtained from the fitting were on the order of ~1 (Table 2). These ratios were corroborated by comparison with experimentally obtained ratios of R_{max} for peptide and small molecule from separate direct binding experiments. These ranged between 0.84 and 1.3 for KN-93 and between 0.8 and 1.1 for calmidazolium. Calculations from these same surfaces show the ratio of ligand activity of Ca^{2+}/CaM for KN-93 and intermediate peptide to also be on the order of 3–4, suggesting that deviations from the expected ratio can be attributed to a stoichiometry of small-molecule binding to Ca^{2+}/CaM that is greater than 1. An estimate of the apparent stoichiometry for KN-93 can be made by noting that $\left[\frac{(R\ \text{max Peptide})}{(R\ \text{max KN93})}\right]\text{Observed} = \left[\frac{(\text{M.W.Peptide})(n1)}{((\text{M.W.KN93})(n2)}\right]$, where n_1 and n_2 represent the stoichiometries of peptide and small-molecule binding to Ca^{2+}/CaM. Since the upper and lower bounds for the fitted ratio of peptide to KN-93 *R*-factor are 1.1–0.9 (Table 2), $1.1–0.9 = \left[\frac{(1984\ \text{Da})(n1)}{(501\ \text{Da})(n2)}\right]$. Assuming that intermediate peptide binds Ca^{2+}/CaM with stoichiometry of 1:1 (i.e., $n_1 = 1$), then $n_2 = 3.6–4.4$. Similar considerations lead to predicted stoichiometries for calmidazolium of 3.4–6. As the confidence interval for the peptide to calmidazolium *R*-factor ratio is not as well defined (Table 2), these predicted stoichiometries should be interpreted with more caution. Finally, samples of Ca^{2+}/CaM prepared for NMR and ITC studies were also tested by SPR. Surface activity calculations from three independent experiments show no significant differences in surface activity between the two preparations. Masses for both preparations were shown to be identical.

NMR sample preparation

A plasmid encoding full-length (residues 1–148) *Rattus norvegicus* CaM was a kind gift from Madeline Shea (University of Iowa). The CaM sequence is identical to the human CaM sequence (Swiss-port code: P62158). Mutations in the CaM gene (M71Q/M72Q/M76Q) and (M109Q/M124Q/M144Q/M145Q) were introduced by site-directed mutagenesis (Roche). Plasmids were verified by DNA sequencing at the Heflin Center for Genomic Sciences at the University of Alabama at Birmingham. Uniformly ^{15}N-labeled and ^{15}N-, ^{13}C-labeled CaM, CaM-N, and CaM-C samples were prepared as described [51,53]. CaM mutants were prepared as described for the wild-type CaM protein. Ca^{2+}/CaM-N protein concentration was measured using bicinchoninic (BCA) protein assay (Thermo Scientific) because it has zero extinction coefficient at 280 nm. The His_8-$CaMKII\delta_{Monomer}$ protein was overexpressed in *E. coli* BL21 (DE3) cells and purified as described [17] with minor modifications. To make a uniformly ^{15}N-labeled His_8-$CaMKII\delta_{Monomer}$ sample, cells were grown in 1L M9 minimal media containing $^{15}NH_4Cl$ at 37 °C until OD_{600} was ~0.8. Cells were then induced

with 1 mM IPTG, grown at 37 °C for ~4 h, spun down, and stored overnight at −80 °C. Next day, the cell pellet was resuspended in 30 mL of lysis/binding buffer containing 50 mM Hepes (pH 7.5), 300 mM NaCl, 20 mM imidazole, and 1× protease inhibitor mix (Protease Inhibitor Cocktail Set I; EMD Millipore). Cells were sonicated, and cell lysate was spun down at 35,000*g* for 30 min. The protein-containing supernatant was purified on nickel affinity resin. The His_8-$CaMKII\delta_{Monomer}$ protein was eluted with a buffer containing 50 mM Hepes (pH 7.5), 300 mM NaCl, 200 mM imidazole, and 1× protease inhibitor mix. The fractions were then pooled and concentrated. Protein was then dephosphorylated with the addition of lambda protein phosphatase (lambda PP; NEB) overnight at 4 °C (dephosphorylation reaction: 400 µL protein at 20 mg/mL, 50 µL 10× NEB buffer, 50 µL 500 mM $MnCl_2$, and 2 µL lambda PP at 400,000 units/mL). Dephosphorylated protein was then applied to Superdex 75 16/60 HiLoad gel filtration column (GE Healthcare) equilibrated with 50 mM Hepes (pH 7.5), 300 mM NaCl, and 10 mM DTT. Fractions were then pooled, concentrated, and washed with NMR buffer [25 mM Tris-d11 (pH 7.0), 100 mM NaCl, 1 mM $CaCl_2$, 10 mM $MgCl_2$, and 1 mM TCEP].

NMR spectroscopy

NMR data were collected at 35 °C on a Bruker Avance II (700 MHz ^1H) and Avance III (600 MHz ^1H) spectrometers equipped with cryogenic triple-resonance probes, processed with NMRPIPE [76], and analyzed with NMRVIEW [77] or CCPN Analysis [78]. CaM, CaM-N, and CaM-C NMR samples were at 100 µM in a buffer containing 25 mM Tris-d11 (pH 7.0), 100 mM NaCl, and 5 mM $CaCl_2$. KN-93 (Calbiochem) used for NMR titrations was prepared in 100% DMSO-d_6 or H_2O at 10–11 mM. Staurosporine was at 10 mM in 100% DMSO-d_6. Signal assignments of Ca^{2+}/CaM are reported elsewhere [50,79]. Signal assignments of methionine methyl signals are in agreement with previous studies [48,49]. The backbone resonances of Ca^{2+}/CaM-N and Ca^{2+}/CaM-C in complex with KN-93 were assigned using standard triple-resonance data (HNCA, HN(CO)CA, HN(CO)CACB, and HNCACB) collected at 35 °C on 500 µM samples in a buffer containing 25 mM Tris-d11 (pH 7.0), 100 mM NaCl, and 5 mM $CaCl_2$. The triple-resonance experiments were collected as non-uniformly sampled sparse data (20% sampling density in indirect dimensions) according to schemes generated using hmsIST [80]. NMR data were processed in NMRPipe [76] in combination with hmsIST programs to reconstruct non-uniformly sampled data [80]. Chemical shift perturbations were calculated as $\Delta\delta_{HN} = \sqrt{\Delta\delta_H^2 + 0.04\Delta\delta_N^2}$, where $\Delta\delta_H$ and $\Delta\delta_N$ are ^1H and ^{15}N chemical shift changes, respectively.

ITC

Thermodynamic parameters of KN-93 binding to Ca^{2+}/CaM or $CaMKII\delta_{Monomer}$ proteins were determined using a MicroCal PEAQ-ITC (Malvern Instruments). Water-soluble KN-93 (Abcam) was used. ITC experiments were conducted in a buffer containing 10 mM Hepes (pH 7.0), 10 mM NaCl, and 1 mM $CaCl_2$. KN-93 at 400 or 411 µM was titrated into 20 or 17 µM of Ca^{2+}/CaM or $CaMKII\delta_{Monomer}$, respectively. Protein concentrations were measured using a Nanodrop (Thermo Fisher Scientific) at a wavelength of 280 nm and using extinction coefficients of 2980 and 45755 M^{-1} cm^{-1} for Ca^{2+}/CaM and $CaMKII\delta_{Monomer}$ proteins, respectively. Heat of reaction was measured at 25 °C for 19 injections. Heat of dilution was measured by titrating KN-93 into buffer and subtracting it from the heat of binding. Data analysis was performed using PEAQ analysis software. Baseline-corrected binding curves were fit using a single set of identical sites to obtain values for K_d, ΔH, and n. Averages and standard deviations of three replicate experiments were used to calculate K_d, ΔH, ΔS, and n.

Analytical ultracentrifugation

Sedimentation velocity experiments for CaMKII FL were performed at 20 °C in a ProteomeLab XL-A analytical ultracentrifuge (Beckman Coulter. Fullerton, CA). Four-hundred-microliter samples of 0.15 µM $CaMKII_{Dodecamer}$ in 25 mM Tris (pH 7.5), 250 mM NaCl, glycerol, and 1 mM TCEP were loaded into a dual-sector charcoal-filled Epon centerpiece. The samples were centrifuged at 40,000 rpm in an An50-Ti rotor, and sedimentation was monitored by absorbance at a wavelength of 280 nm. Data were analyzed with the program SEDFIT (NIH, Bethesda, MD), which generates a continuous distribution or ($c(s)$) for the sedimenting species [81]. The program SEDNTERP [82] was used to estimate the partial specific volume of the proteins as well as the density and viscosity of the buffer solution.

Accession numbers

NMR chemical shift assignments of Ca^{2+}/CaM-N and Ca^{2+}/CaM-C in complex with KN-93 have been deposited in the Biological Magnetic Resonance Data Bank with accession numbers 27712 and 27711 for CaM-N and CaM-C, respectively.

Acknowledgments

We thank David Myszka, Scott Klakamp, Mohammed Youssef, Bruno Marchand, and Ching-Pin Chang for reviewing the manuscript and also

Dharmaraj Samuel, Leanna Lagpacan, and Perry Weissburg for technical assistance. We also thank the Department of Microbiology at the University of Alabama at Birmingham for supporting the project. We thank the comprehensive cancer center at the University of Alabama at Birmingham (funded by the National Institutes of Health grant P30 CA013148) for supporting the High-Field NMR facility.

Conflict of Interest: M.W., N.N., M.L., A.N.M., J. Y.F., D.O.K., K.M.B., H.J.K., B.E.S., R.S., and G.A. P. performed this work as employees of, and with funding from, Gilead Sciences, Inc.

Appendix A. Supplementary data

Supplementary data to this article can be found online at https://doi.org/10.1016/j.jmb.2019.02.001.

Received 20 September 2018;
Received in revised form 14 December 2018;
Accepted 4 February 2019
Available online 10 February 2019

Keywords:
calmodulin;
CaMKII;
calmidazolium;
KN-93;
KN-92

†M.W. and A.B.S. contributed equally to this work.

Abbreviations used:
CaM, calmodulin; Ca^{2+}/CaM, calcium–calmodulin; CaMKII, calmodulin-dependent protein kinase II; SPR, surface plasmon resonance; ITC, isothermal titration calorimetry; HSQC, heteronuclear single quantum coherence; TCEP, tris(2-carboxyethyl)phosphine; EGTA, ethylene glycol-bis(β-aminoethyl ether)-*N*,*N*,*N*′,*N*′-tetraacetic acid; DMSO, dimethyl sulfoxide.

References

[1] M.T. Swulius, M.N. Waxham, Ca(2+)/calmodulin-dependent protein kinases, Cell. Mol. Life Sci. 65 (2008) 2637–2657.
[2] G.A. Wayman, H. Tokumitsu, M.A. Davare, T.R. Soderling, Analysis of CaM-kinase signaling in cells, Cell Calcium 50 (2011) 1–8.
[3] R.M. Tombes, M.O. Faison, J.M. Turbeville, Organization and evolution of multifunctional Ca(2+)/CaM-dependent protein kinase genes, Gene 322 (2003) 17–31.
[4] B.C. Shonesy, N. Jalan-Sakrikar, V.S. Cavener, R.J. Colbran, CaMKII: a molecular substrate for synaptic plasticity and memory, Prog. Mol. Biol. Transl. Sci. 122 (2014) 61–87.
[5] C.H. Thompson, N.A. Hawkins, J.A. Kearney, A.L. George Jr., CaMKII modulates sodium current in neurons from epileptic Scn2a mutant mice, Proc. Natl. Acad. Sci. U. S. A. 114 (2017) 1696–1701.
[6] K.M. Woolfrey, H. O'Leary, D.J. Goodell, H.R. Robertson, E. A. Horne, S.J. Coultrap, et al., CaMKII regulates the depalmitoylation and synaptic removal of the scaffold protein AKAP79/150 to mediate structural long-term depression, J. Biol. Chem. 293 (2018) 1551–1567.
[7] J. Heijman, N. Voigt, X.H. Wehrens, D. Dobrev, Calcium dysregulation in atrial fibrillation: the role of CaMKII, Front. Pharmacol. 5 (2014) 30.
[8] O.O. Mesubi, M.E. Anderson, Atrial remodelling in atrial fibrillation: CaMKII as a nodal proarrhythmic signal, Cardiovasc. Res. 109 (2016) 542–557.
[9] M.Y. Mollova, H.A. Katus, J. Backs, Regulation of CaMKII signaling in cardiovascular disease, Front. Pharmacol. 6 (2015) 178.
[10] R. Zhang, M.S. Khoo, Y. Wu, Y. Yang, C.E. Grueter, G. Ni, et al., Calmodulin kinase II inhibition protects against structural heart disease, Nat. Med. 11 (2005) 409–417.
[11] M.L. Joiner, O.M. Koval, J. Li, B.J. He, C. Allamargot, Z. Gao, et al., CaMKII determines mitochondrial stress responses in heart, Nature 491 (2012) 269–273.
[12] M. Vila-Petroff, M.A. Salas, M. Said, C.A. Valverde, L. Sapia, E. Portiansky, et al., CaMKII inhibition protects against necrosis and apoptosis in irreversible ischemia-reperfusion injury, Cardiovasc. Res. 73 (2007) 689–698.
[13] P. Pellicena, H. Schulman, CaMKII inhibitors: from research tools to therapeutic agents, Front. Pharmacol. 5 (2014) 21.
[14] L.H. Chao, M.M. Stratton, I.H. Lee, O.S. Rosenberg, J. Levitz, D.J. Mandell, et al., A mechanism for tunable autoinhibition in the structure of a human Ca^{2+}/calmodulin-dependent kinase II holoenzyme, Cell 146 (2011) 732–745.
[15] T.R. Gaertner, S.J. Kolodziej, D. Wang, R. Kobayashi, J.M. Koomen, J.K. Stoops, et al., Comparative analyses of the three-dimensional structures and enzymatic properties of alpha, beta, gamma and delta isoforms of Ca^{2+}–calmodulin-dependent protein kinase II, J. Biol. Chem. 279 (2004) 12484–12494.
[16] S.J. Kolodziej, A. Hudmon, M.N. Waxham, J.K. Stoops, Three-dimensional reconstructions of calcium/calmodulin-dependent (CaM) kinase IIalpha and truncated CaM kinase IIalpha reveal a unique organization for its structural core and functional domains, J. Biol. Chem. 275 (2000) 14354–14359.
[17] P. Rellos, A.C. Pike, F.H. Niesen, E. Salah, W.H. Lee, F. von Delft, et al., Structure of the CaMKIIdelta/calmodulin complex reveals the molecular mechanism of CaMKII kinase activation, PLoS Biol. 8 (2010) e1000426.
[18] L. Hoffman, R.A. Stein, R.J. Colbran, H.S. McHaourab, Conformational changes underlying calcium/calmodulin-dependent protein kinase II activation, EMBO J. 30 (2011) 1251–1262.
[19] T. Meyer, P.I. Hanson, L. Stryer, H. Schulman, Calmodulin trapping by calcium–calmodulin-dependent protein kinase, Science 256 (1992) 1199–1202.
[20] A. Forest, M.T. Swulius, J.K. Tse, J.M. Bradshaw, T. Gaertner, M.N. Waxham, Role of the N- and C-lobes of calmodulin in the activation of Ca(2+)/calmodulin-dependent protein kinase II, Biochemistry 47 (2008) 10587–10599.
[21] M. Sumi, K. Kiuchi, T. Ishikawa, A. Ishii, M. Hagiwara, T. Nagatsu, et al., The newly synthesized selective Ca^{2+}/calmodulin dependent protein kinase II inhibitor KN-93 reduces dopamine contents in PC12h cells, Biochem. Biophys. Res. Commun. 181 (1991) 968–975.

[22] H. Hidaka, M. Asano, S. Iwadare, I. Matsumoto, T. Totsuka, N. Aoki, A novel vascular relaxing agent, *N*-(6-aminohexyl)-5-chloro-1-naphthalensulfonamide which affects vascular smooth muscle actomyosin, J. Pharmacol. Exp. Ther. 207 (1978) 8–15.
[23] H. Hidaka, T. Yamaki, M. Asano, T. Totsuka, Involvement of calcium in cyclic nucleotide metabolism in human vascular smooth muscle, Blood Vessels 15 (1978) 55–64.
[24] H. Hidaka, T. Yamaki, M. Naka, T. Tanaka, H. Hayashi, R. Kobayashi, Calcium-regulated modulator protein interacting agents inhibit smooth muscle calcium-stimulated protein kinase and ATPase, Mol. Pharmacol. 17 (1980) 66–72.
[25] H. Hidaka, M. Inagaki, S. Kawamoto, Y. Sasaki, Isoquinolinesulfonamides, novel and potent inhibitors of cyclic nucleotide dependent protein kinase and protein kinase C, Biochemistry 23 (1984) 5036–5041.
[26] H. Tokumitsu, T. Chijiwa, M. Hagiwara, A. Mizutani, M. Terasawa, H. Hidaka, KN-62, 1-[*N,O*-bis(5-isoquinolinesulfonyl)-*N*-methyl-L-tyrosyl]-4-phenylpiperazine, a specific inhibitor of Ca^{2+}/calmodulin-dependent protein kinase II, J. Biol. Chem. 265 (1990) 4315–4320.
[27] H. Yokokura, Y. Okada, O. Terada, H. Hidaka, HMN-709, a chlorobenzenesulfonamide derivative, is a new membrane-permeable calmodulin antagonist, Jpn. J. Pharmacol. 72 (1996) 127–135.
[28] J.D. Johnson, L.A. Wittenauer, A fluorescent calmodulin that reports the binding of hydrophobic inhibitory ligands, Biochem. J. 211 (1983) 473–479.
[29] D.G. Reid, L.K. MacLachlan, K. Gajjar, M. Voyle, R.J. King, England P.J. , A proton nuclear magnetic resonance and molecular modeling study of calmidazolium (R24571) binding to calmodulin and skeletal muscle troponin C, J. Biol. Chem. 265 (1990) 9744–9753.
[30] H. Van Belle, R 24571: a potent inhibitor of calmodulin-activated enzymes, Cell Calcium 2 (1981) 483–494.
[31] W.J. Cook, L.J. Walter, M.R. Walter, Drug binding by calmodulin: crystal structure of a calmodulin–trifluoperazine complex, Biochemistry 33 (1994) 15259–15265.
[32] M. Vandonselaar, R.A. Hickie, J.W. Quail, L.T. Delbaere, Trifluoperazine-induced conformational change in Ca(2+)-calmodulin, Nat. Struct. Biol. 1 (1994) 795–801.
[33] B.G. Vertessy, V. Harmat, Z. Bocskei, G. Naray-Szabo, F. Orosz, J. Ovadi, Simultaneous binding of drugs with different chemical structures to Ca^{2+}–calmodulin: crystallographic and spectroscopic studies, Biochemistry 37 (1998) 15300–15310.
[34] R.M. Tombes, S. Grant, E.H. Westin, G. Krystal, G1 cell cycle arrest and apoptosis are induced in NIH 3T3 cells by KN-93, an inhibitor of CaMK-II (the multifunctional Ca2+/CaM kinase), Cell Growth Differ. 6 (1995) 1063–1070.
[35] H.E. Driessen, V.J. Bourgonje, T.A. van Veen, M.A. Vos, New antiarrhythmic targets to control intracellular calcium handling, Neth. Hear. J. 22 (2014) 198–213.
[36] M.E. Anderson, A.P. Braun, Y. Wu, T. Lu, Y. Wu, H. Schulman, et al., KN-93, an inhibitor of multifunctional Ca^{+} $^{+}$/calmodulin-dependent protein kinase, decreases early afterdepolarizations in rabbit heart, J. Pharmacol. Exp. Ther. 287 (1998) 996–1006.
[37] S. Tessier, P. Karczewski, E.G. Krause, Y. Pansard, C. Acar, M. Lang-Lazdunski, et al., Regulation of the transient outward K(+) current by Ca(2+)/calmodulin-dependent protein kinases II in human atrial myocytes, Circ. Res. 85 (1999) 810–819.
[38] Y. Wu, L.B. MacMillan, R.B. McNeill, R.J. Colbran, M.E. Anderson, CaM kinase augments cardiac L-type Ca^{2+} current: a cellular mechanism for long Q-T arrhythmias, Am. J. Phys. 276 (1999) H2168–H2178.
[39] M.W. Karaman, S. Herrgard, D.K. Treiber, P. Gallant, C.E. Atteridge, B.T. Campbell, et al., A quantitative analysis of kinase inhibitor selectivity, Nat. Biotechnol. 26 (2008) 127–132.
[40] J.K. Tse, A.M. Giannetti, J.M. Bradshaw, Thermodynamics of calmodulin trapping by Ca^{2+}/calmodulin-dependent protein kinase II: subpicomolar Kd determined using competition titration calorimetry, Biochemistry 46 (2007) 4017–4027.
[41] M.N. Waxham, A.L. Tsai, J.A. Putkey, A mechanism for calmodulin (CaM) trapping by CaM-kinase II defined by a family of CaM-binding peptides, J. Biol. Chem. 273 (1998) 17579–17584.
[42] R. Dagher, C. Briere, M. Feve, M. Zeniou, C. Pigault, C. Mazars, et al., Calcium fingerprints induced by calmodulin interactors in eukaryotic cells, Biochim. Biophys. Acta 1793 (2009) 1068–1077.
[43] M.D. Feldkamp, S.E. O'Donnell, L. Yu, M.A. Shea, Allosteric effects of the antipsychotic drug trifluoperazine on the energetics of calcium binding by calmodulin, Proteins 78 (2010) 2265–2282.
[44] M.D. Feldkamp, L. Gakhar, N. Pandey, M.A. Shea, Opposing orientations of the anti-psychotic drug trifluoperazine selected by alternate conformations of M144 in calmodulin, Proteins 83 (2015) 989–996.
[45] A.P. Yamniuk, H.J. Vogel, Calmodulin's flexibility allows for promiscuity in its interactions with target proteins and peptides, Mol. Biotechnol. 27 (2004) 33–57.
[46] K.T. O'Neil, W.F. DeGrado, How calmodulin binds its targets: sequence independent recognition of amphiphilic α-helices, Trends Biochem. Sci. 15 (1990) 59–64.
[47] T. Yuan, H. Ouyang, H.J. Vogel, Surface exposure of the methionine side chains of calmodulin in solution. A nitroxide spin label and two-dimensional NMR study, J. Biol. Chem. 274 (1999) 8411–8420.
[48] K. Siivari, M. Zhang, A.G. Palmer III, H.J. Vogel, NMR studies of the methionine methyl groups in calmodulin, FEBS Lett. 366 (1995) 104–108.
[49] M. Osawa, M.B. Swindells, J. Tanikawa, T. Tanaka, T. Mase, T. Furuya, et al., Solution structure of calmodulin–W-7 complex: the basis of diversity in molecular recognition, J. Mol. Biol. 276 (1998) 165–176.
[50] R.H. Ghanam, T.F. Fernandez, E.L. Fledderman, J.S. Saad, Binding of calmodulin to the HIV-1 matrix protein triggers myristate exposure, J. Biol. Chem. 285 (2010) 41911–41920.
[51] A.B. Samal, R.H. Ghanam, T.F. Fernandez, E.B. Monroe, J. S. Saad, NMR, biophysical, and biochemical studies reveal the minimal calmodulin binding domain of the HIV-1 matrix protein, J. Biol. Chem. 286 (2011) 33533–33543.
[52] C. Agamasu, R.H. Ghanam, J.S. Saad, Structural and biophysical characterization of the interactions between calmodulin and the Pleckstrin homology domain of Akt, J. Biol. Chem. 290 (2015) 27403–27413.
[53] T.F. Fernandez, A.B. Samal, G.J. Bedwell, Y. Chen, J.S. Saad, Structural and biophysical characterization of the interactions between the death domain of Fas receptor and calmodulin, J. Biol. Chem. 288 (2013) 21898–21908.
[54] B.J. Chang, A.B. Samal, J. Vlach, T.F. Fernandez, D. Brooke, P.E. Prevelige Jr., et al., Identification of the calmodulin-binding domains of Fas death receptor, PLoS One 11 (2016) e0146493.

[55] E.M. Balog, L.E. Norton, R.A. Bloomquist, R.L. Cornea, D.J. Black, C.F. Louis, et al., Calmodulin oxidation and methionine to glutamine substitutions reveal methionine residues critical for functional interaction with ryanodine receptor-1, J. Biol. Chem. 278 (2003) 15615–15621.
[56] D. Chin, A.R. Means, Methionine to glutamine substitutions in the C-terminal domain of calmodulin impair the activation of three protein kinases, J. Biol. Chem. 271 (1996) 30465–30471.
[57] W.C. Prozialeck, B. Weiss, Inhibition of calmodulin by phenothiazines and related drugs: structure–activity relationships, J. Pharmacol. Exp. Ther. 222 (1982) 509–516.
[58] E. Stenberg, B. Perssson, H. Roos, C. Urbaniczky, Quantitative determination of surface concentration of protein with surface plasmon resonance using radiolabeled proteins, J. Colloid Interface Sci. 143 (1991) 513–526.
[59] T.M. Davis, W.D. Wilson, Determination of the refractive index increments of small molecules for correction of surface plasmon resonance data, Anal. Biochem. 284 (2000) 348–353.
[60] A.W. Drake, M.L. Tang, G.A. Papalia, G. Landes, M. Haak-Frendscho, S.L. Klakamp, Biacore surface matrix effects on the binding kinetics and affinity of an antigen/antibody complex, Anal. Biochem. 429 (2012) 58–69.
[61] M. Ben-Johny, I.E. Dick, L. Sang, W.B. Limpitikul, P.W. Kang, J. Niu, et al., Towards a unified theory of calmodulin regulation (calmodulation) of voltage-gated calcium and sodium channels, Curr. Mol. Pharmacol. 8 (2015) 188–205.
[62] M. Weinreuter, M.M. Kreusser, J. Beckendorf, F.C. Schreiter, F. Leuschner, L.H. Lehmann, et al., CaM kinase II mediates maladaptive post-infarct remodeling and pro-inflammatory chemoattractant signaling but not acute myocardial ischemia/reperfusion injury, EMBO Mol Med. 6 (2014) 1231–1245.
[63] J. Backs, T. Backs, S. Neef, M.M. Kreusser, L.H. Lehmann, D.M. Patrick, et al., The delta isoform of CaM kinase II is required for pathological cardiac hypertrophy and remodeling after pressure overload, Proc. Natl. Acad. Sci. U. S. A. 106 (2009) 2342–2347.
[64] A. Roy, J. Ye, F. Deng, Q.J. Wang, Protein kinase D signaling in cancer: a friend or foe? Biochim. Biophys. Acta 1868 (2017) 283–294.
[65] A. Hudmon, H. Schulman, Structure-function of the multifunctional Ca^{2+}/calmodulin-dependent protein kinase II, Biochem. J. 364 (2002) 593–611.
[66] L. Gao, L.A. Blair, J. Marshall, CaMKII-independent effects of KN93 and its inactive analog KN92: reversible inhibition of L-type calcium channels, Biochem. Biophys. Res. Commun. 345 (2006) 1606–1610.
[67] S. Rezazadeh, T.W. Claydon, D. Fedida, KN-93 (2-[*N*-(2-hydroxyethyl)]-*N*-(4-methoxybenzenesulfonyl)amino-*N*-(4-chlorocinnamyl)-*N*-methylbenzylamine), a calcium/calmodulin-dependent protein kinase II inhibitor, is a direct extracellular blocker of voltage-gated potassium channels, J. Pharmacol. Exp. Ther. 317 (2006) 292–299.
[68] D.O. Koltun, E.Q. Parkhill, R. Kalla, T.D. Perry, E. Elzein, X. Li, et al., Discovery of potent and selective inhibitors of calmodulin-dependent kinase II (CaMKII), Bioorg. Med. Chem. Lett. 28 (2018) 541–546.
[69] G. Papalia, D. Myszka, Exploring minimal biotinylation conditions for biosensor analysis using capture chips, Anal. Biochem. 403 (2010) 30–35.
[70] D.G. Myszka, T.A. Morton, CLAMP: a biosensor kinetic data analysis program, Trends Biochem. Sci. 23 (1998) 149–150.
[71] R. Karlsson, Affinity analysis of non-steady-state data obtained under mass transport limited conditions using BIAcore technology, J. Mol. Recognit. 12 (1999) 285–292.
[72] T.A. Morton, D.G. Myszka, Kinetic analysis of macromolecular interactions using surface plasmon resonance biosensors, Methods Enzymol. 295 (1998) 268–294.
[73] D.G. Myszka, X. He, M. Dembo, T.A. Morton, B. Goldstein, Extending the range of rate constants available from BIACORE: interpreting mass transport-influenced binding data, Biophys. J. 75 (1998) 583–594.
[74] C. Crauste, N. Willand, B. Villemagne, M. Flipo, E. Willery, X. Carette, et al., Unconventional surface plasmon resonance signals reveal quantitative inhibition of transcriptional repressor EthR by synthetic ligands, Anal. Biochem. 452 (2014) 54–66.
[75] M. Geitmann, K. Retra, G.E. de Kloe, E. Homan, A.B. Smit, I. J. de Esch, et al., Interaction kinetic and structural dynamic analysis of ligand binding to acetylcholine-binding protein, Biochemistry 49 (2010) 8143–8154.
[76] F. Delaglio, S. Grzesiek, G.W. Vuister, G. Zhu, J. Pfeifer, A. Bax, NMRPipe: a multidimensional spectral processing system based on UNIX pipes, J. Biomol. NMR 6 (1995) 277–293.
[77] B.A. Johnson, R.A. Blevins, NMR view: a computer program for the visualization and analysis of NMR data, J. Biomol. NMR 4 (1994) 603–614.
[78] W.F. Vranken, W. Boucher, T.J. Stevens, R.H. Fogh, A. Pajon, M. Llinas, et al., The CCPN data model for NMR spectroscopy: development of a software pipeline, Proteins 59 (2005) 687–696.
[79] M. Ikura, L.E. Kay, A. Bax, A novel approach for sequential assignment of 1H, 13C, and 15N spectra of proteins: heteronuclear triple-resonance three-dimensional NMR spectroscopy. Application to calmodulin, Biochemistry 29 (1990) 4659–4667.
[80] S.G. Hyberts, A.G. Milbradt, A.B. Wagner, H. Arthanari, G. Wagner, Application of iterative soft thresholding for fast reconstruction of NMR data non-uniformly sampled with multidimensional Poisson Gap scheduling, J. Biomol. NMR 52 (2012) 315–327.
[81] P. Schuck, Size-distribution analysis of macromolecules by sedimentation velocity ultracentrifugation and lamm equation modeling, Biophys. J. 78 (2000) 1606–1619.
[82] T. Laue, B. Shah, T. Ridgeway, S. Pelletier, Computer-aided interpretation of analytical sedimentation data for proteins, in: S.E. Harding, A.J. Rowe, J.C. Horton (Eds.), Analytical Ultracentrifugation in Biochemistry and Polymer Science, Royal Society of Chemistry, Cambridge 1992, p. 90.